Gorguze Family Laboratory
2609 Draper Dr.
Ann Arbor, MI 48109
April 23, 2021

Professors Timothy Smith and George Halow
Aerospace 495 Laboratory
François-Xavier Bagnoud Building
1320 Beal Ave.
Ann Arbor, MI 48109

Subject: Final Report Transmittal for Development of Modular Dynamometer and Thrust Test Stand

Dear Doctor Timothy Smith and Professor George Halow,

Attached is the final report of our development of a modular thrust test stand and electric motor dynamometer which is capable of testing electric aircraft motors with propeller diameters ranging from 5 to 22 inches. The test stand is capable of recording motor torque, thrust, and power consumption of the motor being tested and outputting all of these measurements for further analysis.

Included in this report are our methods for successfully developing, constructing, testing, and validating our test stand, initial calibration of all of our sensors, and initial test data for three known motor and propeller combinations. With the resources that have been allocated to this team, both financial and otherwise, we have been able to successfully complete the first stage of this project while remaining within the allocated budget.

The thrust test stand satisfies two of three of our success criteria as it has demonstrated its feasibility and reliability through initial testing, but does not meet our expectations to be considered effective. We have found that there are still limitations with the current implementation of our design, notably our torque measurement is subject to hysteresis under large or sustained torque loading. Additionally, the load cell that was procured for this project, while extremely consistent in all load cases, seems to have durability issues as we have had two of them fail without reaching their load rating.

Future work for this project includes procuring a load cell that can last the life of the system, which we expect to be on the order of ten to twenty years of regular use, identifying necessary issues with the remote-control of the software, finding a hardware solution to the torque measurement hysteresis, and ensuring that the system reliably saves data to an SD card.

Thank you for your support of our project during this term and we are pleased to report the success of our modular dynamometer and thrust test stand.

Sincerely,

Cameron Gable   Hogan Hsu   Sergio Ramirez Sabogal   Anthony Russo   Brian Sandor

FINAL REPORT

DEVELOPMENT OF MODULAR DYNAMOMETER AND THRUST TEST STAND

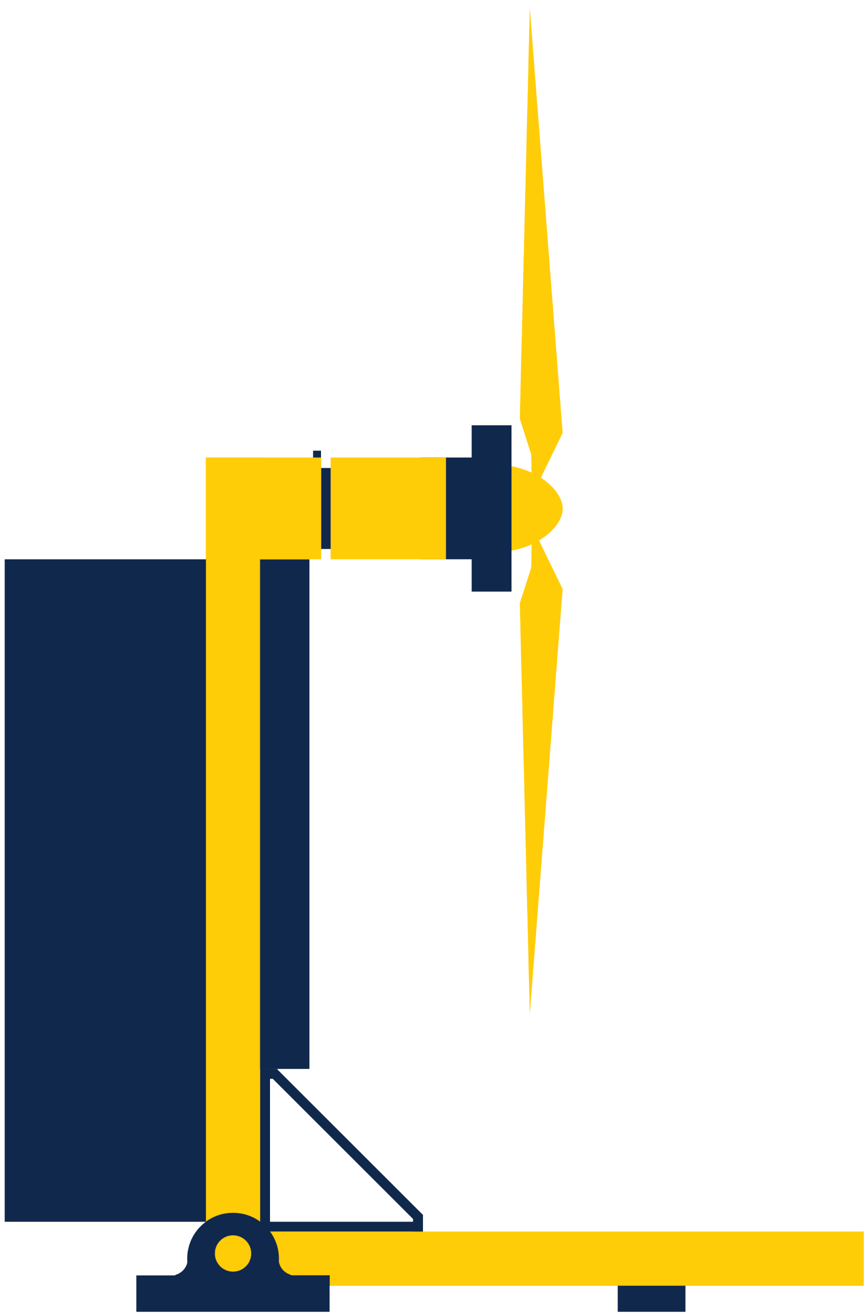

FINAL REPORT

DEVELOPMENT OF MODULAR DYNAMOMETER AND THRUST TEST STAND

April 23, 2021

Project Engineers:

Cameron Gable
Hogan Hsu
Anthony Russo
Sergio Ramirez Sabogal
Brian Sandor

Project Sponsor:

Professor George F. Halow

Contents

List of Figures

List of Tables

I. Executive Summary

Electric motors and propellers come in an extremely large variety, and varying the combinations of motors and propellers will result in different levels of performance. A number of student teams are currently participating in the *Aerospace 495 Systems Engineering Leadership Course* taught by Professor George F. Halow. These teams are creating quadcopter drone racers (Michigan Drone Racing), an electric vertical take-off and landing aircraft (Michigan Vertical Flight Technology), and a conventional take-off and landing aircraft (MACH). All of these teams need to test their propulsion systems to ensure their motor and propeller combinations meet the needs of their architecture. As such, Professor Halow has tasked us with designing, building, and testing a modular electric motor dynamometer and thrust test stand capable of covering the range of motor and propeller requirements that are covered in the Aerospace 495 course. This report describes the design, calibration, and testing of the thrust test stand.

Over the semester, our team of engineers has designed, analyzed, assembled, and tested the modular dynamometer and thrust test stand. The design is capable of measuring thrust, torque, and power of electric motors and propellers ranging from 5-22 inches in diameter. The design also includes environmental sensors for temperature and pressure and was progressed for future implementation of RPM and pitot-static measurement.

Currently, our design shows promising results for all success criteria, all of which are defined below. Our thrust stand design partially satisfies our effectiveness criterion as during our initial testing, we were able to compare our thrust results to those tested by MVFT and found that maximum thrust was within 5% of the previously measured value. However, our current and power measurements were roughly 10% larger than the known values, so we cannot say that aspect is effective. It is recommended to reevaluate the power measurements to increase precision and accuracy to become effective. Additionally, we were unable to implement the RPM sensor into the stand due to its complexity and our timeline.

As for reliability, we were able to show that using the same motor and propeller combination over multiple trials, our test stand reported very consistent and repeatable results. This was also shown to be the case over our calibration efforts where all metrics showed remarkable consistency. Much like the previous criterion, we recommend further testing to confidently claim reliability of the system but given the large amounts of data that we have collected thus far, we are confident that the system will continue to be reliable.

Finally, we can confidently say that our system meets our criterion of feasibility. The system has been built and run multiple times with great success, and is able to accommodate propellers ranging from 5 inches to 22 inches. Through computational testing, we can confidently say that the system will not fail under the loads and stresses of any of the motors it is capable of supporting and we can conclude that this criterion is met with no need for further testing although further testing and usage will only confirm this to be the case.

II. Introduction

Electric remote control aircraft are a cornerstone of a comprehensive aerospace engineering education due to their accessibility and ability to be designed, built, tested, and flown by students. A crucial component of these aircraft is their electric propulsion system which generally consists of electric motors and propellers. Being able to accurately and precisely test these propellers is absolutely crucial to ensuring the successful design of a propulsion system for aircraft. Unfortunately, electric motors and propellers come in a large variety of sizes, making testing different motor and propeller combinations tricky, as most thrust test stands and dynamometers are rated for a specific propeller size. Our team set out to develop a modular dynamometer and thrust test stand that will be able to measure thrust, torque, and RPM for a propeller and motors ranging from 5-22 inches in diameter. In this document, we introduce the potential benefits and impact of our product and describe the motivation behind this project. We describe our design for the stand and detail the experimentation and testing done to validate its results. We also break down our costs and schedule of this project.

A. Defining the Problem and Benefits

Multiple student project teams are currently taking part in *Aerospace 495 Systems Engineering Leadership Course* taught by Professor George F. Halow, where they are tasked with projects such as creating quadcopter drone racing vehicles. Currently, the teams involved need to spend time, energy, and resources to develop individually sized test stands to gather accurate measurements on their electric motor and propeller propulsion systems. By developing a modular dynamometer and thrust test stand set up that can accommodate the full range of motor and propeller combinations utilized by the teams, we can alleviate the need for students to design, build, and test their own thrust stands.

As mentioned above, this thrust test stand is able to accommodate propellers with diameters ranging from 5 inches to greater than 20 inches. This is a capability that is not offered by off-the-shelf test stands which often have much smaller ranges or are specifically for much larger propellers. This allows this stand to test motors for a very large range of electric aircraft. Specifically, this range was selected to allow for all electric aircraft design teams at the University of Michigan College of Engineering to be able to use this test stand.

In addition to the highly modular design, our test stand uses a fully custom-made data collection suite which will allow all motor measurements to be taken autonomously and saved directly to a micro SD Card for analysis. This data collection suite is also equipped with pre-loaded test campaigns available at the touch of a button, eliminating the need for direct operation of the test campaigns and allowing the user(s) to directly monitor the health of the motors during operation. This test stand will also be more affordable than its off-the-shelf counterparts. It is also be designed for manufacturability allowing it to be easily repairable and adaptable for years into the future.

To summarize, the major impacts this test stand will have are in providing project teams an accurate, highly versatile piece of test equipment that is not available elsewhere. There are several benefits of this design over similar models in the industry. First is in price, as the industry standard test stands cost significantly more than the budget utilized to create this product. The next is in versatility as no model available is able to accurately test motor/propeller combinations over the range of this one and there was no research found covering highly versatile thrust measurement for small electric motors.

B. Previous and Current Research

Thrust stands able to measure thrust, RPM, motor torque, and power draw have been previously built and can be bought off the shelf [1]. However, existing off-the-shelf thrust stands are normally lower quality in construction and cost significantly more than building a custom stand. Researchers have developed propeller thrust stands and dynamometers for various configurations and propeller sizes. However, many of these designs are either developed specifically for smaller propellers between 3 and 10 inches [2], or for propellers 10 inches and larger [3]. While they serve their purpose, these solutions have not been characterized for the full range of propeller sizes that we are interesting in evaluating. As a result, they do not offer the modularity that we hope to achieve in our system.

That being said, while research will not not directly solve our identified problem, it still provides valuable insight towards various aspects of our project. This includes different sensor equipment and techniques for measuring thrust, torque, and RPM. Additionally, in the papers by Hossain and Li, they both provide extensive descriptions of the methods used to calibrate both their thrust and torque sensors, which was helpful to determine our own calibration methodology [2, 4].

C. Task Details

Multiple designs were explored and analyzed using computer-aided design modelling, finite-element analysis (FEA), and computational fluid dynamics (CFD) to determine the optimal thrust stand design. From there, higher fidelity CFD and FEA simulations were performed to ensure that the chosen design could handle the expected maximum loads. Various parts were then procured, machined, and assembled. Next, we calibrate all the various sensors on the stand. This also includes integrating all software and electrical components to properly read, store, and display data. We then tested the stand on various known motor and propeller combinations to validate its accuracy and precision. This data is used to make any final adjustments to the stand.

III. Criteria

Our design, build, and test of the modular dynamometer and thrust test stand is guided by three main criteria. These criteria are utilized to assess all the data and results from our analyses and experiments, and ultimately determine the success of the system. These criteria are effectiveness, reliability, and feasibility.

A. Effectiveness

The most important criterion for our project is effectiveness, which includes its ability to accurately measure thrust, torque, and power. To be considered effective, we require that our thrust stand to generate results within 5% of the expected data for each propeller. To ensure accurate measurements, work needs to be done to validate that the results read from our stand match expected thrusts and torques from known motor and propeller combinations. To do so, experimental testing of known motor and propeller combinations is necessary so see how our stand compares to manufacturer specifications. This criterion must be met in order for thrust stand to be trusted and useful to future project teams and students.

B. Reliability
Another important criterion for our project is the reliability of the results and how repeatable each experiment is. The benchmark for this criterion is that results and curves from our calibration be within the 95% confidence interval of the mean data across multiple tests of the same configuration in the same environment. In order to determine the reliability of our system, the same experiments were run multiple times to ensure that our stand is measuring similar values every time the same experiment is performed.

C. Feasibility
The feasibility of our test stand is determined by its modularity and ability to test a range of motor and propeller sizes. Ability to test a wide range and variety of motor and propeller sizes is necessary to verify that our thrust stand can effectively accommodate propellers ranging from 5-22 inches in diameter.

Another goal of the feasibility criterion is that the thrust stand can withstand the maximum expected loads that it will see. This is addressed both by computational analyses and experimental testing to verify the thrust stand can withstand the expected maximum loads of 20 lbf of thrust and 15 lbf-in of torque.

IV. Design
Our thrust stand has been designed with modularity as the main objective. It features two interchangeable vertical arm lengths shown in Figure 1, allowing for testing to occur for a variety of propeller and motor sizes. This also allows for the thrust stand to operate in both large and small wind tunnels, making test scheduling more convenient for the users. These arms were manufactured and assembled out of 80/20 t-slotted aluminum extrusion which is both cheap and easy to assemble. Our design employs the classic L-shape thrust stand concept, with a load cell slotted under the horizontal arm. A bearing pivot is located where the two arms of the stand meet, allowing for free rotation around that axis. As the propeller thrusts forward, the entire assembly rotates about the pivot, engaging the load cell.

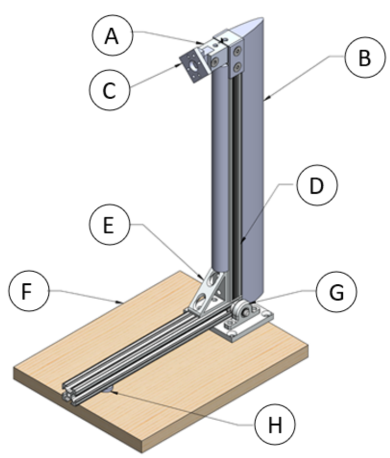

A	Flexure Pivot
B	Aerodynamic Fairing
C	Motor Mount
D	Vertical Arm (11 or 14 in.)
E	Corner Brace
F	Base Board
G	Bearing Pivot
H	50-lb Load Cell

Fig. 1 Thrust stand design

Our motor mounting plates allow for the mounting of various motors with different bolt patterns. The various sizes of these plates allow for testing on small motors and large motors on the same stand. Our unique flexure torque measurement device allows for torque data to be collected from all ranges of motor sizes that fit on the thrust testing stand. This innovation increases the effectiveness and accuracy of the data from other more traditional torque measurement solutions. These system design choices increase the effectiveness of our thrust stand and allow it to meet a wide variety of the user's testing needs.

A. Flexure/Motor Mount Assembly

To measure the torque of tested motors, we constructed a custom spring mechanism shown in Figure 2. The idea behind this is to use a precision flexure pivot with a known spring constant and measure the displacement angle to calculate the torque. This design acts as a motor mount on the rotating side of the mechanism, as well as an attachment point to the frame on the fixed side.

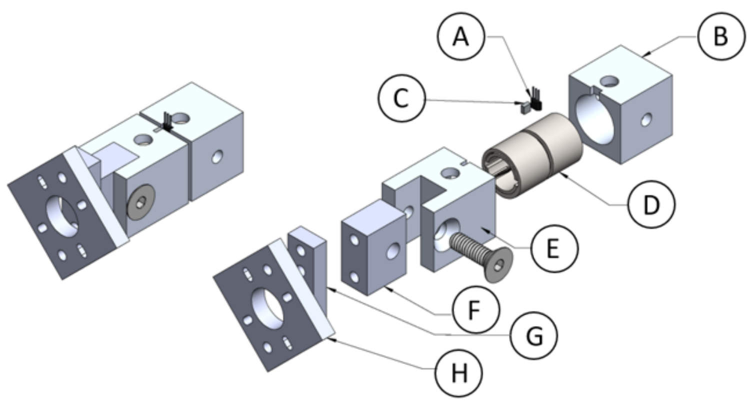

A	Hall Effect Sensor
B	Fixed Mount
C	1/16" Thick Neodymium Magnet
D	Ø ¾" Flexure Pivot
E	Rotating Mount
F	Motor Mount Key
G	Large Motor Mount Adapter
H	Large Motor Mount

Fig. 2 Assembled and exploded view of the torque measurement mechanism

For this design, we used a flexure pivot with a spring constant of 3.261 lbf-in/degree. Based on specs from the maximum size motor we anticipate being tested, the torque on the thrust stand should not exceed 15 lbf-in, meaning we should never exceed 4.6° of angular displacement. To measure this angle, we use a small hall sensor mounted on the fixed side of the pivot that reads the poles of a thin neodymium magnet mounted on the rotating side of the pivot. Since the hall sensor reads a 5 V signal on one pole and 0 V on the other, we achieve 10-bit resolution between either side of the magnet when using the Arduino Mega's analogRead() function.[5][6] This provides us with a full measurement range based on the thickness of the magnet. For the longevity of the pivot, the manufacturer [7] supplies life projections of their flexure pivots based on the axial and torsional loads shown in Figure 3.

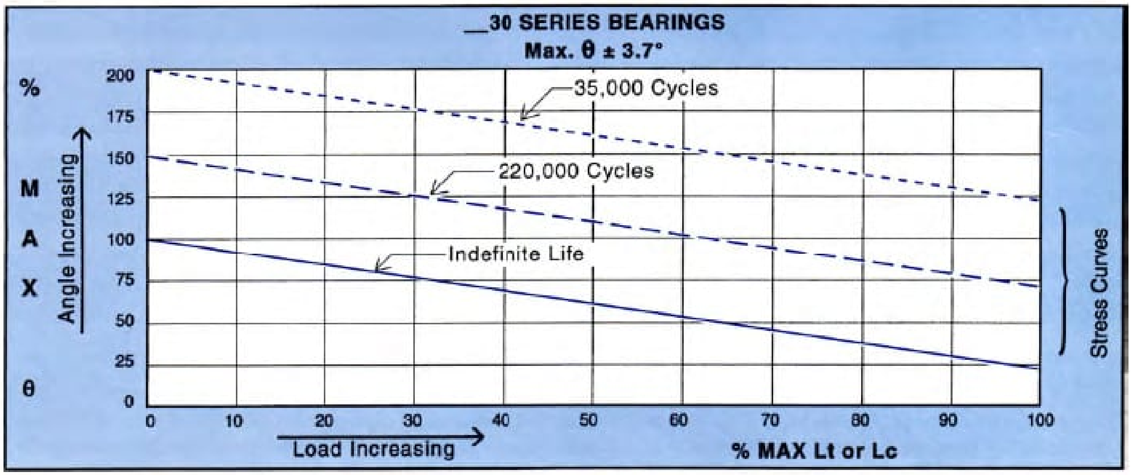

Fig. 3 Expected life cycle of flexure pivot [7]

With this life expectancy curve, we expect to be well within the 220,000 cycle range since only our largest motor will reach 125% of the recommended maximum angle for indefinite life of the flexure. Additionally, we expect to be low on the axial loading on the horizontal axis since the flexure is rated for 900 lbs. As a result, we expect the torque measurement system to last for a nearly indefinite amount of time, depending on usage of the thrust stand. Also, once the flexure fails, it can simply be removed from the mounts and a new one can be installed in its place.

B. Aerodynamic Fairing

As seen in Figure 1 the vertical arm of the test stand is equipped with fairings on the forward and aft side to streamline flow around the structure. These fairings can be seen in Figure 4. In addition to the fairings, the remaining exposed slots of the 80/20 aluminum extrusion have filler strip to prevent additional flow disturbances along the sides. After preliminary CFD analysis, is was determined that the test stand would benefit greatly from a symmetric airfoil type fairing during dynamic testing in wind tunnels.

The decision was made to go forward with a NACA 0015 airfoil fit to the structure. This choice was made due to the airfoil's combination of low drag coefficient at reasonable testing condition Reynolds numbers ranging from 50,000 to 175,000 [8], as well as the ability to fit to the structure relatively flush without protruding too far forward, into the propeller blade plane. The Reynolds number is a non-dimensional ratio of inertial forces to viscous forces used to aid in fluid flow analysis. By using our range of propeller diameters along with the potential wind tunnel testing speeds, we were able to calculate this range of testing condition Reynolds numbers. The rear fairing also serves as a conduit for the wiring to the RPM and torque sensors to securely feed from the top of the test stand down to the base.

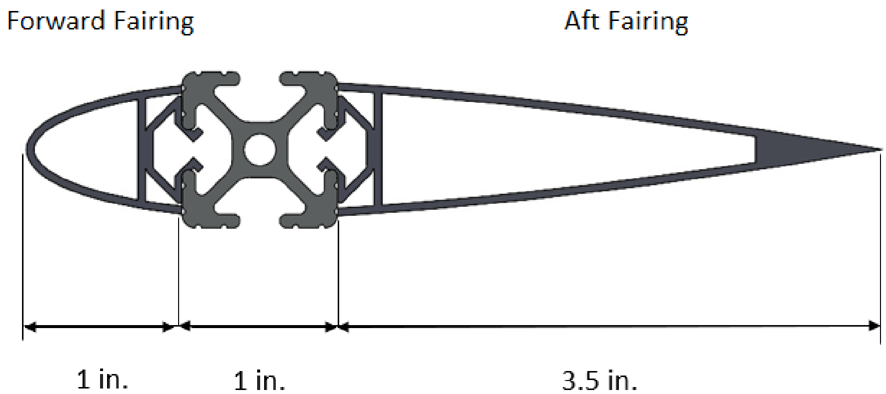

Fig. 4 Cross-sectional view of the vertical arm with forward and aft fairings as seen from above test stand looking down. All lips between fairing and structure are 0.08 inches

C. Hardware

The brain of the thrust stand is the base station powered by an Arduino Mega microcontroller. The Arduino Mega was selected for its large number of I/O pins. These allow us to use a variety of sensors to collect the important data from the tests. The data is collected by a carefully selected variety of sensors. These sensors include a load cell to measure thrust, a current and voltage sensor to record power use, a custom reflective tachometer to record motor RPM, a custom flexure based torque sensor, and a temperature sensor to record environmental data. This data is written to a micro SD card via an SD card module attached to the Arduino Mega. This allows for the data to be easily recorded and extracted from the thrust stand for further analysis. Due to safety concerns it was necessary to remove the user from the vicinity of the large spinning propellers. The solution to this was to create an additional remote unit from an Arduino Nano microcontroller seen below in Figure 5.

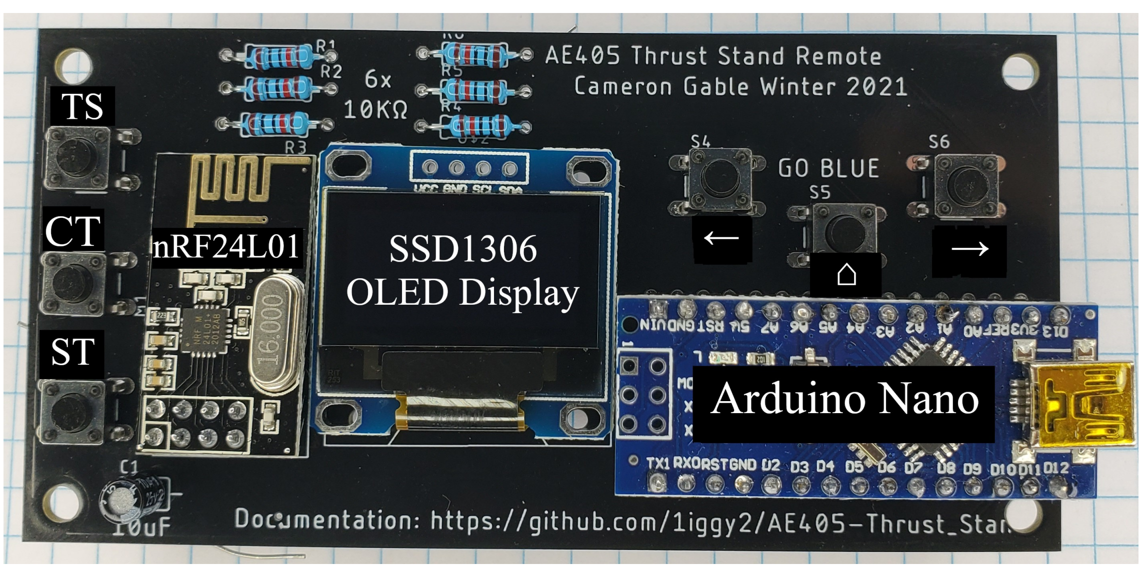

Fig. 5 Assembled PCB of Remote Circuit

Six buttons are used for user input this allows us to select and start the test to be performed while removed from the danger zone. A small SSD1306 OLED display is installed on the controller to provide feedback to the user on their test parameter selections. The base station and remote communicate using the nRF24L01 2.4 GHz radio transceiver module. This allows the user to be removed up to 100 meters (328 feet) from the testing area. The remote also has an emergency stop functionality built into it. If the test is not continuing ideally the user can press a single button and send a kill signal to the base station, ending the test. Of course it is not wise to rely on a single point of failure, and a way to manually disconnect power safely from a distance is also provided.

A printed circuit board was designed and manufactured to allow for simple construction of the remote. This allows for duplicates to be easily constructed in case a remote is lost or damaged. The electrical connections for the base station are illustrated in Appendix A Figure 15, and the electrical connections for the remote are shown in Appendix A Figure 16. A 3D printable case was designed to cover the remote printed circuit. It is shown below in Figure 6.

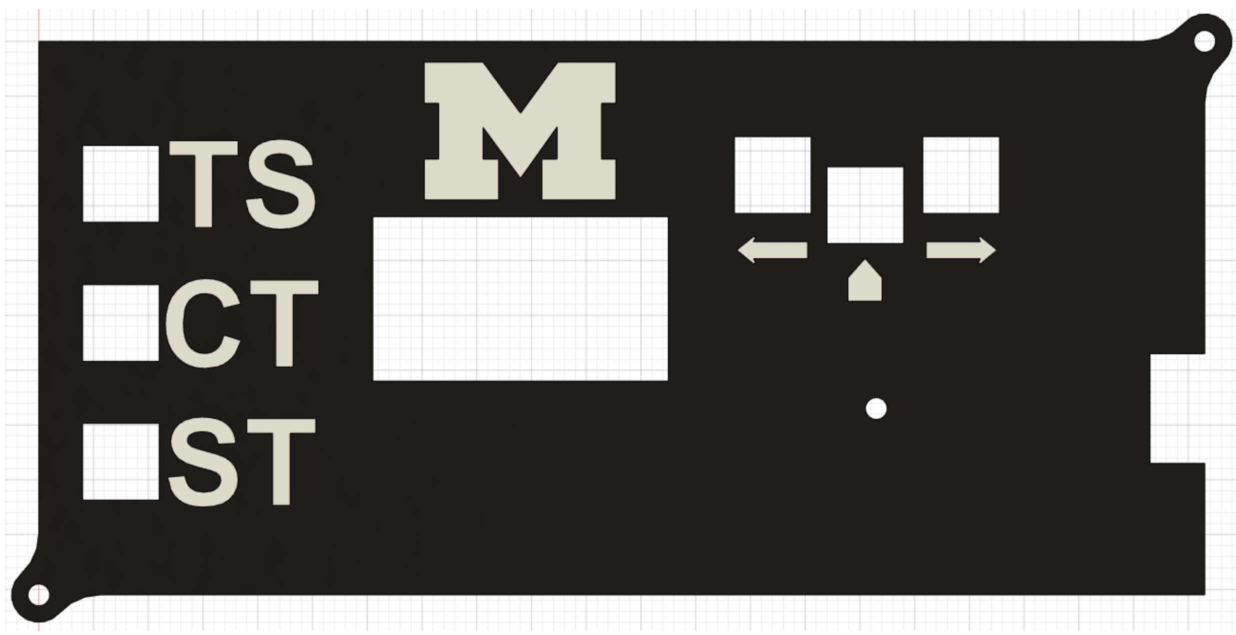

Fig. 6 Face of 3D Printable Remote Case

D. Software

The software to complement our hardware suite is written in the Arduino coding language, that is based on C++. The code is written with extensive helper functions and comments to increase human readability of the code. To start the software development process, flowcharts were created for both the base station and remote. This helped lay out the architecture of the code and resulted in a smoother development experience. The flowchart for the remote and base station software is seen in the appendix as Appendix B Figure 17 and Appendix B Figure 18.

We initially thought we would need to use the new microcontroller from Raspberry Pi, the Pico. However, a little known library for our SSD1306 OLED display was discovered. It reduced the

RAM overhead of the display and only allows for text to be displayed on the SSD1306. This allowed for the development to continue using the Arduino Nano programmed in C++ language rather than the less common and less supported MicroPython language. Another breakthrough was to replace the initially proposed KY-040 Rotary Encoder for three buttons for remote graphical user interface navigation. This removed the RAM overhead from the KY-040 library and also allowed for the Arduino Nano to be used. Consistent radio communication between the remote and base station have been tested and are working as intended. This was a major step in the development as the ability to be a safe distance from the thrust testing was a major requirement.

The data recorded by our sensors is saved to a text file through the MicroSD card breakout board+ by Adafruit. This allows for easy data extraction, and analysis. The stretch goal of development of a program to analyze the data remains as future work to be completed. Data extraction is as simple as using the import function of Google Sheets. The result of a raw file import seen below in Figure 7. Testing data files are saved with dynamically iterative names to ensure that no data is lost or overwritten during testing.

	A	B	C	D	E	F
1	AE405 Thrust Stand		Winter 2021			
2	Cameron Gable	Hogan Hsu	Anthony Russo			
3	Brian Sandor	Sergio Ramirez Sabogal				
4						
5	Find Documentation at:		https://github.com/1iggy2/AE405-Thrust_Stand			
6						
7	Ambient Conditions:					
8	Temperature:	20.31	Celsius			
9	Pressure:	98485.11	Pascals			
10						
11	Throttle	Time (ms)	Thrust (N)	Volts	Amps	Torque (in-lb)
12	1000	0	0.03	12.52	0.2	0.87
13	1000	20	0.02	12.6	0.41	0.87
14	1000	32	0.02	12.6	0.41	0.87

Fig. 7 Imported Testing Data

The software supports three types of thrust tests. They are named Throttle Sweep, Constant Throttle, and Stress Test. Throttle Sweep tests take in user inputs consisting of a starting throttle, ending throttle, total test time, and step time. The software calculates the necessary throttle jumps to complete the test in the given bounds. This test is suspected to be the most useful as it allows for the characterization of motor performance at various different throttle settings. Constant Throttle tests take in a throttle value and test time. The thrust stand runs the motor at the given value for the given time allowing for testing of the motor at specific throttle settings for a range of times. Stress Tests take in a high throttle value, low throttle value, total test time, and switching time. This test allows for testing motor performance in highly dynamic environments. This allows the user to test if motor performance and efficiency are deteriorated by rapid changing throttle settings. These performance inputs can be checked against the menu number packet system by using the chart seen in Table 1 below. A description of the menu number packet system and the user input process can be seen in Appendix B Figure 17.

Parameter	Description	Throttle Sweep	Constant Throttle	Stress Test
A	Test Type	1	2	3
BBB	Primary Throttle	Starting Throttle	Throttle	High Throttle
CCC	Secondary Throttle	Ending Throttle	N/A	Low Throttle
DDD	Test Time	Total Test Time	Total Test Time	Total Test Time
EEE	Step Time	Step Time	N/A	Switching Time

Table 1 Menu Number Value Description

We have been using our team Github page for version control and have been documenting our design decisions. This page acts as an instruction manual and repair guide for our sponsor and future users. This is also used to document and justify our design decisions, along with keeping track of the required features for sponsor delivery. The instruction manual begins with important safety considerations and examples. As the safety was our sponsors primary concern we found it very important to put additional emphasis on this point. The GitHub link has been immortalized on the remote printed circuit board silkscreen seen in Figure 5. This should allow the users to find the repository, read the instructions, troubleshoot issues, and request support even after all team members have graduated. It also will enable future work to continue to be documented after the submission of the final report, allowing future work to benefit the sponsor if the project is continued. The documentation is available on GitHub at:

`https://github.com/1iggy2/AE405-Thrust_Stand`

V. Support

Our modular propeller dynamometer and thrust test stand is designed to be effective, feasible, and reliable. These three criteria are analyzed and their support is discussed below.

A. Support for Effectiveness

To test the effectiveness of our thrust stand, we tested three different motor/propeller combinations and compared them with past data. Unfortunately, there is no manufacturer data on the motor and propellers we tested, but we have data from tests conducted by MVFT two years ago. This does not entirely verify our data since the tests conducted by MVFT have their own degree of uncertainty in accuracy, but we wanted to see if the results were comparable to determine if we were in the ballpark. All tests were performed using the Lumenier ZIP 2407-1750 kV motor, Xilo 40A ESC, and Lumenier 4s 5300 mAh battery. This best replicated the original testing conditions of the original MVFT tests and only the propeller was varied. Results from our tests and the MVFT tests are shown in Table 2.

Propeller	Max Thrust (Meas.) (lbf)	Max Current (Meas.) (A)	Max Thrust (MVFT) (lbf)	Max Current (MVFT) (A)
5.1x3.1x3	1.7	17.4	1.8	15.2
6x4	2.3	21.5	2.4	19.2
5x5.3x3	1.7	17.8	1.8	14.9

Table 2 Comparison of MVFT results to results from testing of modular test stand

From Table 2 you can see that our maximum thrust values measured with our thrust stand get very close to the maximum thrust values of the MVFT measured data. However, our maximum current seems to go higher for every propeller.

In Figures 8, 9, 10 below, we show static thrust data for three different motor and propeller combinations. In these tests, the throttle setting on the motor was swept from 0 – 100% through a 100 second test, with 5% throttle steps every 5 seconds.

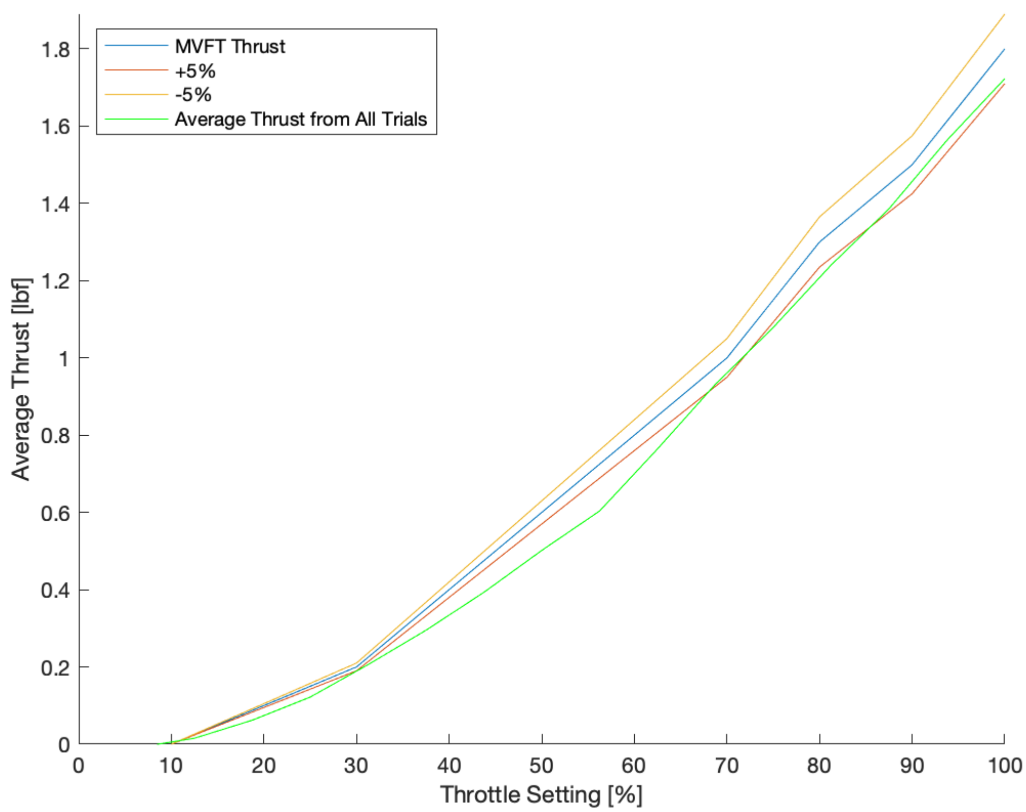

Fig. 8 Average Thrust vs. Throttle setting comparison, 5.1x3.1x3 Prop

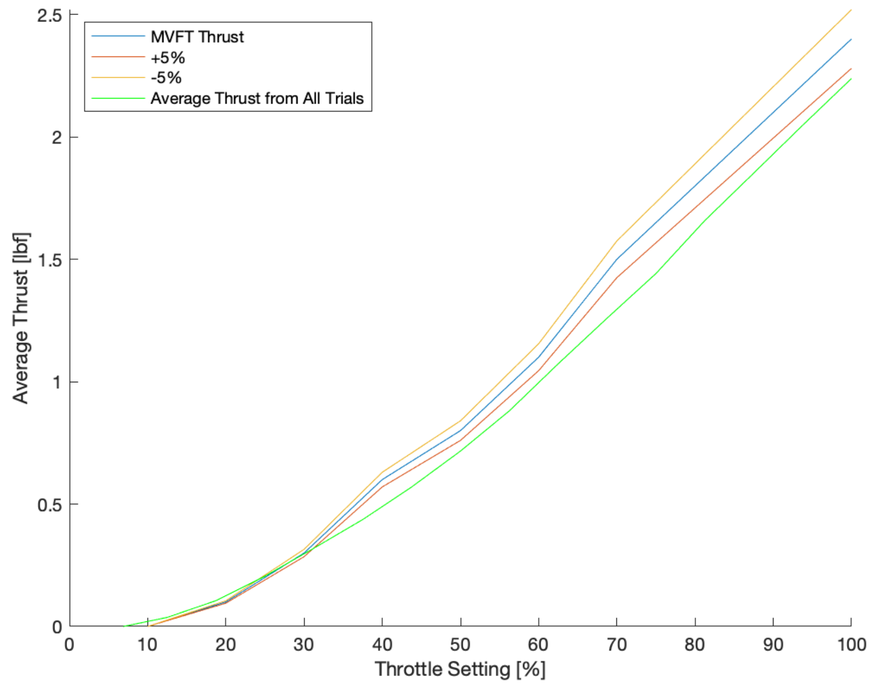

Fig. 9 Average Thrust vs. Throttle setting comparison, 6x4 Prop

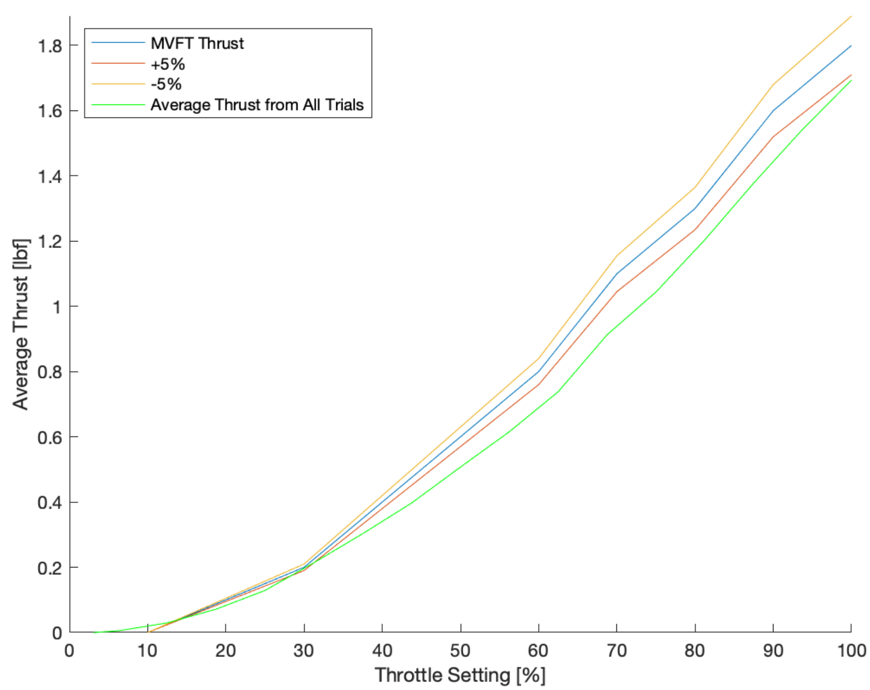

Fig. 10 Average Thrust vs. Throttle setting comparison, 5x5.3x3 Prop

We can see that the results for thrust were comparable to the results from MVFT. Figures 8, 9, and 10 show that our average values over all our tests for each configuration tend to be lower than those reported by MVFT. While this may be an issue with the effectiveness of our thrust stand in reporting thrust values, it could also be an issue with the thrust stand created by MVFT. We can take away from these figures, however, that our trends are very similar and we can expect that after further investigation, the results from the two systems may converge. However, based on the load cell calibration results shown in Figure **??**, we believe our results from the modular thrust stand are more accurate than the tests performed by MVFT. The MVFT propulsion lead did inform us that MVFT did not fully calibrate their system before testing and recording data. The torque, voltage, and current data, as well as the raw data for the thrust from these tests can be seen in Appendix D in Figure 21 - 32. MVFT did not gather data for these other parameters, and so it is difficult to determine the effectiveness of our stand in those measurements.

B. Support for Reliability

To test the reliability of the thrust stand, we first needed to determine the reliability of the sensor suite measuring all the data. Calibration of our sensors was performed by setting the measured parameter to a known value and then recording the raw output from the respective sensor. This was performed three separate times for each sensor calibration, shown in Figure 11. A more detailed explanation of our sensor calibration procedure can be found in Appendix C. In each of the plots in Figure 12, the x-axis is the raw output from the sensor and the y-axis is the measured parameter. The average of the three trials was plotted and the error bars were determined by taking the 95% confidence interval using a student's t-distribution.

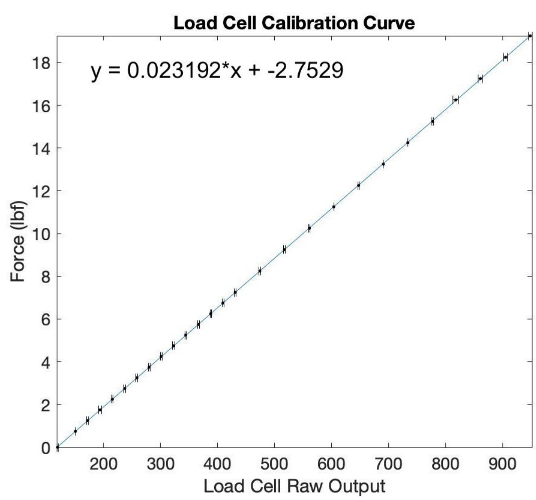

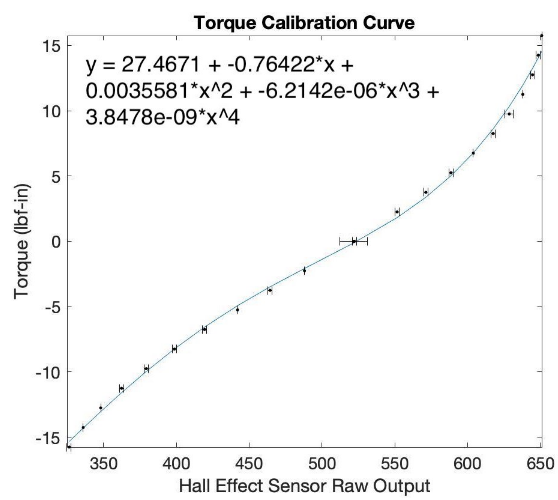

Fig. 11 Load Cell, Torque, Calibration Curves and Equations

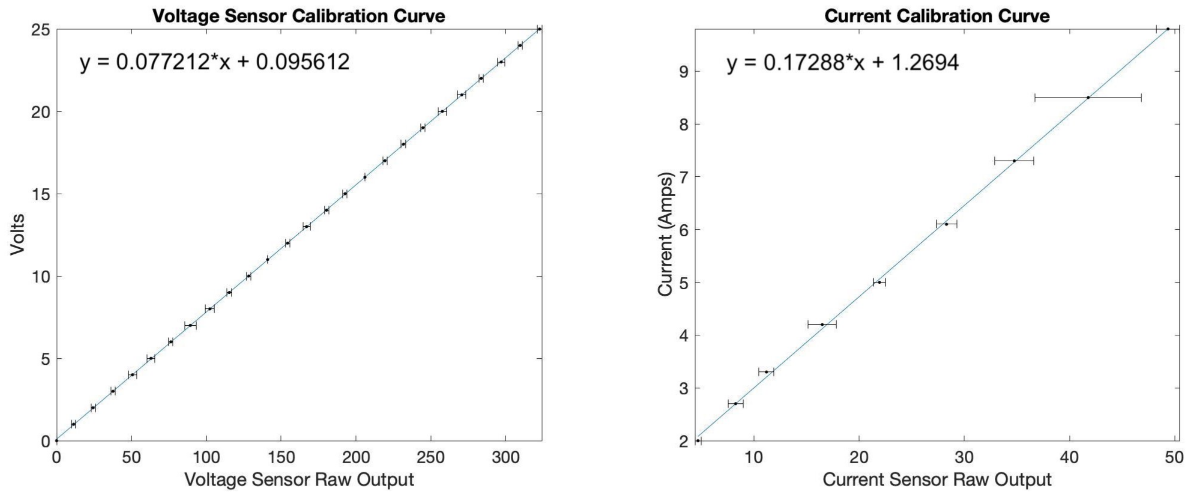

Fig. 12 Voltage, Current Calibration Curves and Equations

From the calibration plots in Figures 11 and 12, you can see that for every sensor, the calibration curve fit to the data falls within the majority of the error bars plotted. On top of that, for most of the error bars, particularly in the load cell and voltage calibrations, the error bars are quite small, meaning that the we can be 95% confident that our output from the sensor will be within that small range. This shows that we were able to get repeatable data across the three trials, indicating that the sensors have reliable performance.

Another important parameter to measure for when analysing the reliability of the system is the hysteresis. This measurable is defined as the systems dependence on its past states. While almost all sensors returned to their natural positions after testing, torque measurements were dependent on previous loading when subject to larger loads. To analyze this phenomenon, we applied a known large torque to either side of the torque calibration mount seen in Appendix C Figure 20 for a one-minute period then recorded the new "zero value" to analyze how much it drifted. These measurements can be found on Table 3. As seen, there is a hysteresis concern when applying torques near the maximum limit of this stand. This will be something to consider for further testing but does not significantly affect our ability to satisfy the reliability requirement.

	Movement of Zero Torque Reading (lbf-in)		
Applied Torque	Trial 1	Trial 2	Trial 3
-11.25	0	-0.0578	-0.1158
11.25	0.0576	0.0578	0.0578
-15.75	-0.0576	-0.1727	-0.1154
15.75	0.1154	0.2307	0.1734

Table 3 Torque Measurement Hysteresis

C. Support for Feasibility

Thrust (lbf)	Torque (lbf-in)	Long Arm Max Stress (MPa)	Short Arm Max Stress (MPa)
20	15.0	105.641	91.098
18	13.5	93.877	81.988
16	12.0	83.446	72.879
14	10.5	73.015	63.769
12	9.0	62.584	54.659
10	7.5	52.154	45.549
8	6.0	41.723	36.439
6	4.5	31.292	27.329
4	3.0	20.861	18.220
2	1.5	10.431	9.110
1	1.0	5.224	4.566

Table 4 Maximum Stress of Both Long and Short Arm FEA Models

The feasibility of the thrust stand depends on its ability to withstand the maximum expected loads. FEA simulations were performed on CAD models for the long and short arm models over the range of expected loads to computationally verify that our design is structurally reliable. The yield strength of aluminum 6105-T5, the material used for our 80/20 aluminum extrusion, is 240 MPa at 23°C [9]. We find this to be a reasonable temperature for our operations, and have used this number as a baseline. From Table 4 above, none of our max stresses from either the long arm or short arm model reach 240 MPa. This increases our confidence in the feasibility of our design, as even our largest max stress in the long arm model still has a safety factor of almost 2.4.

To further support this, during the calibration process of both the load cell, a maximum load of 19.25 lbf and 12.25 lbf was placed on the long arm and short arm configurations respectively. While doing this, the thrust stand remained structurally stable and did not displace in any significant or noticeable fashion. Similarly, when calibrating the hall effect sensor in the flexure assembly, a maximum torque of 15.75 lbf-in was applied to the head of the stand. By applying these loading conditions multiple times, the stand design has shown that it can withstand the maximum loading conditions for the two different arm configurations.

Finally, our thrust stand design has been built to accommodate the full range of propellers. This can be seen in Figure 33 and 34 in Appendix E.

The feasibility of the test stand is also dependent on the reliability of the hardware. This is of particular interest given the aforementioned issues with the load cell. The load cell broke after very minimal use. While no further issues are expected with the more simple components that make up the other sensing elements, we can not determine that the product is feasible until the problem with the load cell is remedied.

VI. Conclusion and Future Steps

Based on the data we gathered from calibration and thrust testing, we can say that we partially met the effectiveness requirement, fully met reliability, and fully met feasibility.

A. Conclusions

We are not able to say that we have met the effectiveness requirement because of significant errors in our current sensor. We found the thrust load cell and voltage sensor to be very accurate in testing and well within 5% of the expected results for each motor we tested. However, the current measurement was generally 10% larger than expected, so we cannot say that our current or power measurements are effective.

We are able to say that we met the reliability requirement. In all of our calibration tests, we found that we could consistently measure the same load within 5% for all our sensors. Additionally, in our static testing, we were able to see that the data from all 3 trials for each configuration were very consistent.

We are also able to say that we met the feasibility requirement. We were able to demonstrate that we could comfortably fit propellers and motors ranging from 5 to 22 inches in diameter to satisfy the size feasibility. To satisfy the loading criteria, we have FEA simulations that demonstrate the structural loading of the stand. Additionally, we applied the full torque and forcing loads to the stand during calibration and found that the stand was capable of supporting our expected loads of 20 lbf and 15 lbf-in.

B. Limitations

Since we were unable to implement the RPM sensor and the airspeed sensor, we are currently limited in the amount of useful parameters we can calculate. Without the RPM sensor, we are unable to calculate the mechanical power which would come from a combination of the RPM and torque measurements. Additionally, we would not be able to nondimensionalize the propeller performance. Similarly, without the airspeed sensor, we would not be able to directly match the airspeed with the other data we collected. Running dynamic tests would require much more involved testing procedures since the airspeed would have to be manually recorded at each wind tunnel setting and need to be matched to each testing file. With the built-in airspeed sensor, we would be able to have continuous airspeed data at each sample and allow us to determine how the propeller responds to changing airspeed.

C. Future Plans

The next step for testing would be to begin dynamic testing of propellers. This would require us to implement and calibrate the RPM and airspeed sensors to provide the capability of calculating dimensionless values of the propellers. To calibrate the RPM sensor, we would have to spin up a motor to a constant RPM and use a separate handheld tachometer to compare the measurements. For the airspeed sensor, we will place the sensor in the wind tunnel and use the manometer to compare the airspeed results.

Additionally, it would be worth investigating new options for the main thrust load cell. The one we purchased for our project was very accurate and repeatable, however, it broke two separate times during testing for seemingly no reason. We properly wired the load cell to our Arduino and it functioned for enough time to gather calibration and static test data, but it failed on our last day of testing. This likely could have been because of the relatively low cost of the load cell compared to others on the market and consequently poor manufacturing. Therefore, we recommend finding a new supplier for a 50-lbf load cell with a separate Wheatstone bridge amplifier. This could potentially be replaced with one of the bar load cells in the 405 lab which have been proven to be much more durable.

To improve the results from the torque sensor, the angular displacement measurement should be improved. During calibration, we found that the displacement was very non-linear and we lost a lot of precision on the higher loads. The manufacturer specifications for the flexure boast very good linearity so we expect it to rotate a constant angle as the load increases. Therefore, we suspect the non-linearity is the result of the hall effect sensor measuring the angular displacement. The magnetic field from the circular magnet is likely not as linear as we assumed, so replacing it with a square magnet with a more constant magnetic field may improve the linearity of the hall effect. Additionally, the entire measurement system could potentially be replaced with a small contact encoder to precisely measure the angular displacement and calculate the torque.

Finally, the main wiring of the base station should be soldered to perfboard or a custom printed circuit board to improve the overall quality of the build. Currently, the entire base station is assembled using a bread board and is susceptible to damage. This would take the current product from a prototype system to a final production product.

VII. Management Plan

At the beginning of the semester we set a feasible budget and schedule in order to track our progress and make sure we would be able to deliver the final product to Professor Halow on time. Throughout the semester, we have regularly met with both the professors of the course as well as Professor Halow himself to update them on our progress, get feedback, and make changes to our design. We have kept to this schedule as best as possible but have experienced some delays which are discussed in more detail below. We were also able to remain within the allocated materials budget. Our full budget breakdown is below.

A. Budget

The budget for this project, as with most engineering projects, was a significant design driver. The expected and actual cost breakdowns for all resources required for this project are shown below in Table 5. From the table, once can note that our largest cost item was our Flexure Pivot with an actual cost of \$118.06, accounting for over a quarter of the overall material budget of %400. This cost was justified as the Flexure Pivot, coupled with a hall effect sensor, will give us a reliable and dependable torque measurement system that will last throughout the life of our thrust test stand. Our next highest cost item was our load cell with an actual cost of \$38.47. Again, this was a justified cost because we determined that this load cell was the most capable and reliable for our application. Finally, the Pillow Block Bearings were the third highest item with an actual cost of \$36.46. These were justified as being the absolute best methods to mitigate static friction concerns on the pivot point of our thrust test stand.

Our three highest-cost items accounted for \$192.99, nearly half of our materials budget, but each were justified to be the absolute best option, with cost considered, for their applications. Outside of materials, our overall highest cost item was engineering labor. Overall, the total labor time is \$32,000 which is approximately 16 hours a week, per engineer, for 10 weeks totaling 800 hours at a standard rate of \$40/hr. Also included in the final budget are a 50% overhead cost and an additional 10% for contingency costs which, as can be seen by our resulting Actual Total, were not used. Our total materials cost was \$354.90 which was \$45.10 below our materials cost.

B. Schedule

Our team made substantial progress but failed to stay on track with the schedule that we set at the beginning of the semester. The schedule for this project is shown in Figures 13 and 14 below. Our slip in schedule was due to a combination of unforeseen circumstances. Notably, our largest hit to the schedule was due to a failure with the initial load cell that we procured from Newark Electronics. This issue meant that we had to get a new one and with a lead time of about a week, this issue set us back one week in our schedule.

Additionally, there were major setbacks in integrating and testing the code and analysis package. Because of these setbacks, and other minor impacts to schedule, we were unable to complete testing with MDR or MACH and we were unable to perform dynamic testing in the wind tunnel. We completed the major goals of the project and have completed a system that is reliable and feasible but, due to schedule constraints, were unable to fully verify its effectiveness. As such, the system is not yet ready for full release and use by the Aerospace 495 Course and thus, we recommend that testing and development continue past this term before the system is fully released.

Category	Item	Expected Cost ($)	Actual Cost ($)
Structural Materials	80/20 T-Slot Aluminum	17.00	17.68
	Mounting Bracket	15.00	9.99
	Pillow Block Bearing	40.00	36.46
	Aluminum Pivot Mount	5.00	5.34
	Flexure Mount	5.00	4.92
	Pivot Shaft	10.00	17.48
	Flexure Pivot	100.00	118.06
	2' x 2' Plywood Base	5.00	1.95
Subtotal		**197.00**	**211.88**
Instrumentation	Load Cell	50.00	38.47
	Current and Voltage Sensor	10.00	19.95
	Temperature Sensor	4.00	14.95
Subtotal		**64.00**	**73.37**
Computing Suite	Microcontroller	40.30	16.99
	MicroSD Card Breakout	7.50	8.49
	LED/OLED Data Screen	17.50	9.99
	Transciever	12.00	11.99
Subtotal		**77.30**	**47.46**
Operating Expenses	Fastners	15.00	9.05
	Calibration Equipment	40.00	0.00
	T-Slot Cover	5.00	4.15
	Reflective Tape	9.00	8.99
Subtotal		**69.00**	**22.19**
Labor	Engineers		32,000.00
Facilities	Labs	0.00	0.00
Overhead		50.00%	16,203.50
Contingency		10.00%	3,240.70
TOTAL		**51,851.20**	**32,354.90**

Table 5 Cost Breakdown by Component

TASK NAME	START DATE	END DATE	DURATION* (WORK DAYS)	PERCENT COMPLETE
Concept Definition				
Establish Initial Concepts	2/2	2/11	9	100%
Create Initial BoM	2/5	2/11	6	100%
Create Initial Financial Budget	2/2	2/9	7	100%
Create Preliminary Schedule	2/2	2/14	12	100%
Trade Concept Designs	2/2	2/15	13	100%
Initial Design				
Start Design (All Systems)	2/15	2/22	7	100%
Preliminary FEA	2/17	2/24	7	100%
Finalize Design	2/24	3/3	7	95%
Finalize Budget	2/18	3/3	13	100%
Prelim Software Development	2/24	3/3	7	100%
Manufacturing				
Develop Initial Manufacturing Plan	3/3	3/10	7	100%
Procure all Materials	2/24	3/10	14	100%
Continue Software Development	3/3	3/15	12	100%
Test Electronics	3/3	3/10	7	100%
Machine Components	3/10	3/25	15	100%
Initial Assembly	3/22	3/29	7	100%
Final Assembly	3/29	4/2	4	100%
Testing and Optimization				
Software Integration	4/2	4/9	7	100%
Software Optimization	4/9	4/16	7	100%
System Calibration	4/2	4/9	7	90%
MDR and MACH Testing	4/9	4/14	5	0%
MVFT Testing	4/9	4/14	5	75%
Final Modifications	4/14	4/16	2	80%
System Readiness Review	4/16	4/17	1	100%
System Ready for Release	4/17	4/19	2	0%
Technical Communication				
Proposal Presentation	2/9	2/25	16	100%
Proposal	2/9	3/2	21	100%
Phase-I Report	3/2	3/9	7	100%
Phase-II Report Draft	3/9	4/1	23	100%
Poster Presentation	4/1	4/15	14	100%
Phase-II Report	4/1	4/23	22	100%

Fig. 13 Project Schedule Details

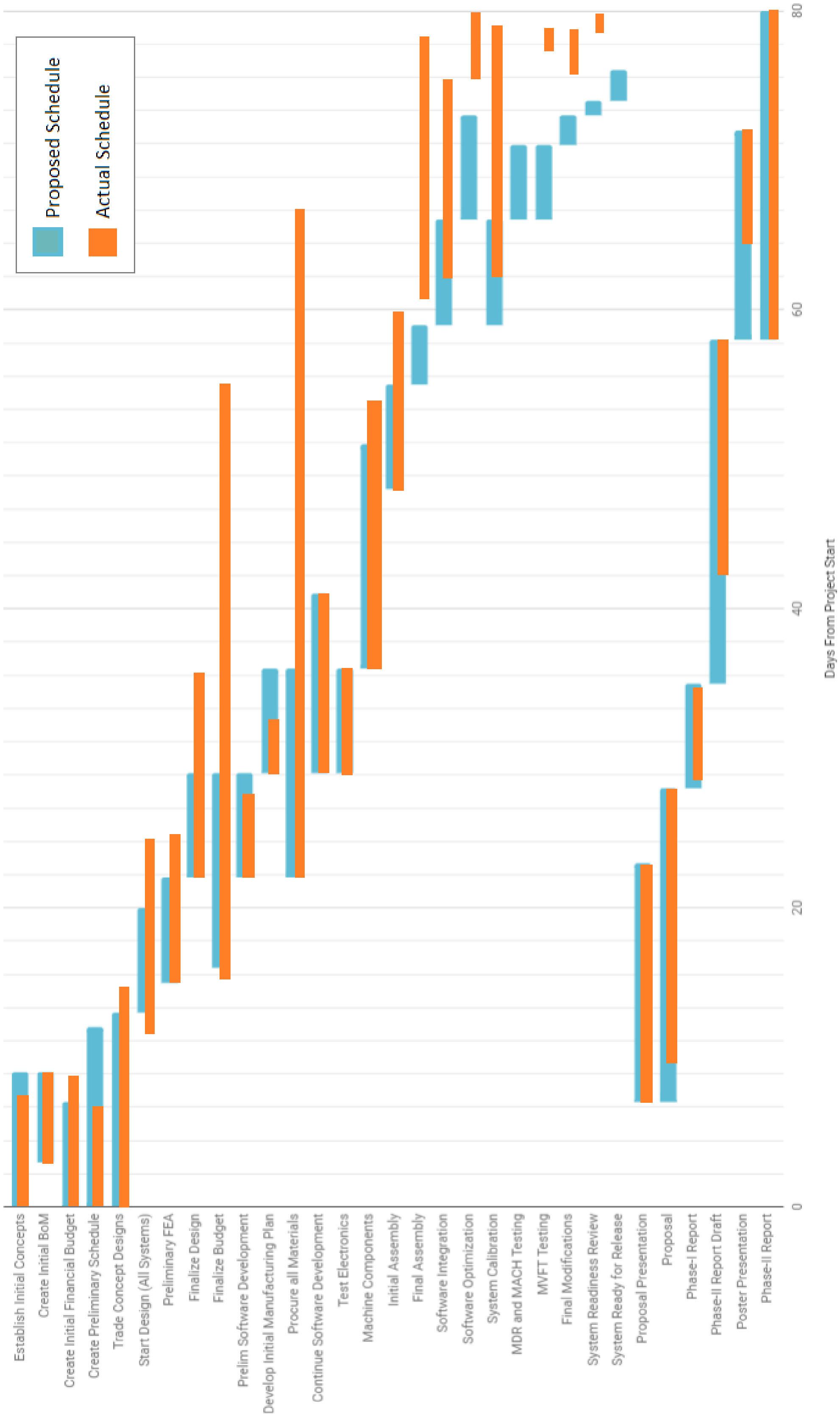

Fig. 14 Project Schedule Bar Chart

References

[1] "Brushless Motor and Propeller Thrust Stands," RCbenchmark Available: https://www.rcbenchmark.com/

[2] Hossain M. R., Krouglicof, N.,"Propeller Dynamometer for Small Unmanned Aerial Vehicle," *CCECE 2010*, 2010. https://ieeexplore.ieee.org/document/5575152

[3] Asson, K. M., Dunn, P. F., "Compact Dynamometer System that Can Accurately Determine Propeller Performance," *Journal of Aircraft*, vol. 29, pp. 8-9, 1992. https://arc-aiaa-org.proxy.lib.umich.edu/doi/abs/10.2514/3.46118

[4] Li, H. H., Davis, K. R., Davy, M. H. Green, S. I. "A Marine Propeller Aerodynamic Test Facility," *Strain*, vol. 43, pp. 125-131, 2007. https://doi-org.proxy.lib.umich.edu/10.1111/j.1475-1305.2007.00325.x

[5] "DIY Flight Simulator Joystick," Tom Stanton Available: https://www.youtube.com/watch?v=SgqflcHBTwc

[6] "Arduino analogRead() Documentation," Arduino Available: https://www.arduino.cc/reference/en/language/functions/analog-io/analogread/

[7] "Life Expectancy of C-Flex Pivot Bearings," C-Flex Bearing Co., Inc. Available: https://c-flex.com/pivot-bearings/life-projections/

[8] "NACA 0015," Airfoil Tools Available: http://airfoiltools.com/airfoil/details?airfoil=naca0015-il

[9] "AA Standards Grade 6105 T5." Matmatch Available: https://matmatch.com/materials/alky16105229t50-aa-standards-grade-6105-t5

VIII. Appendix

A. Hardware Diagrams

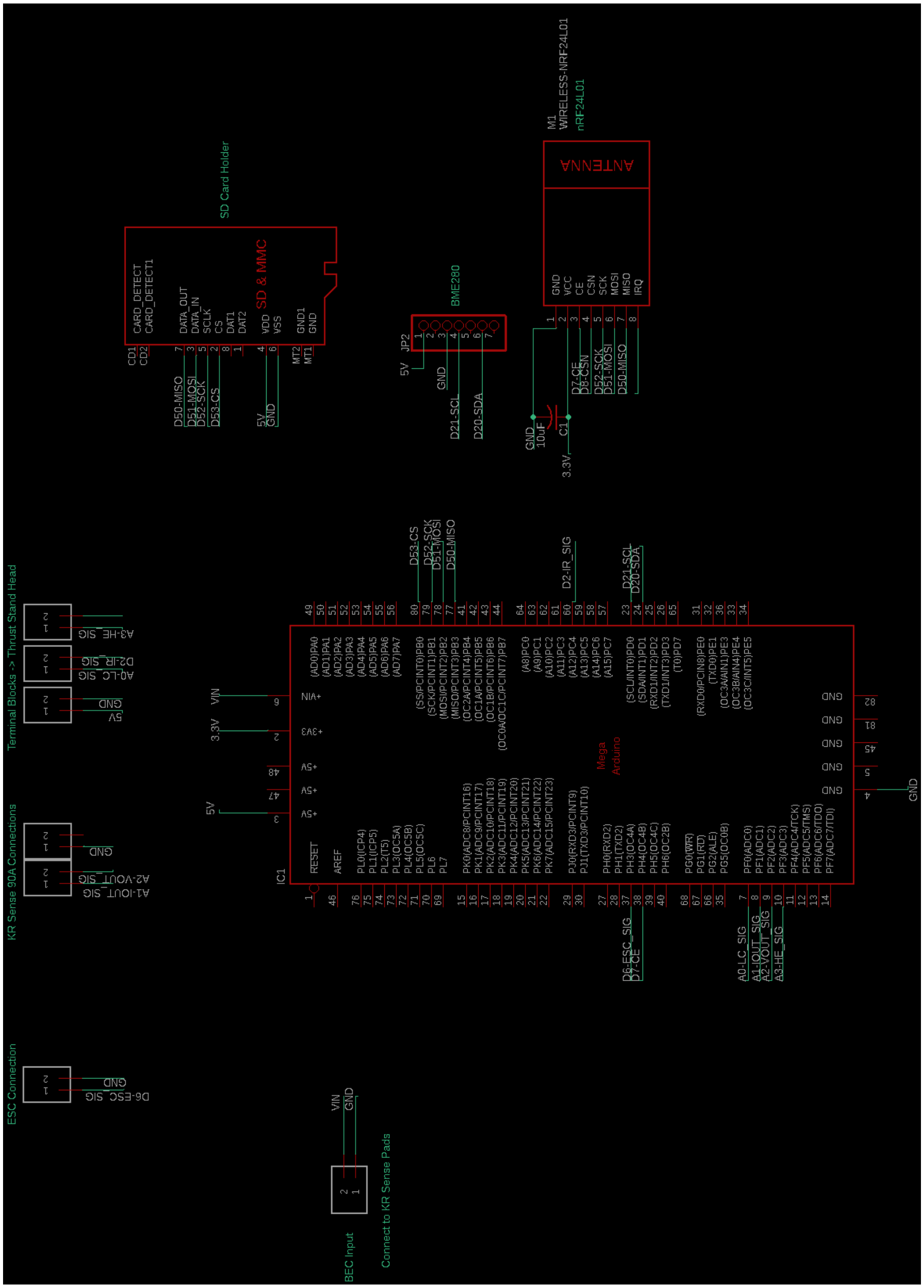

Fig. 15 Base Station EAGLE Connection Diagram

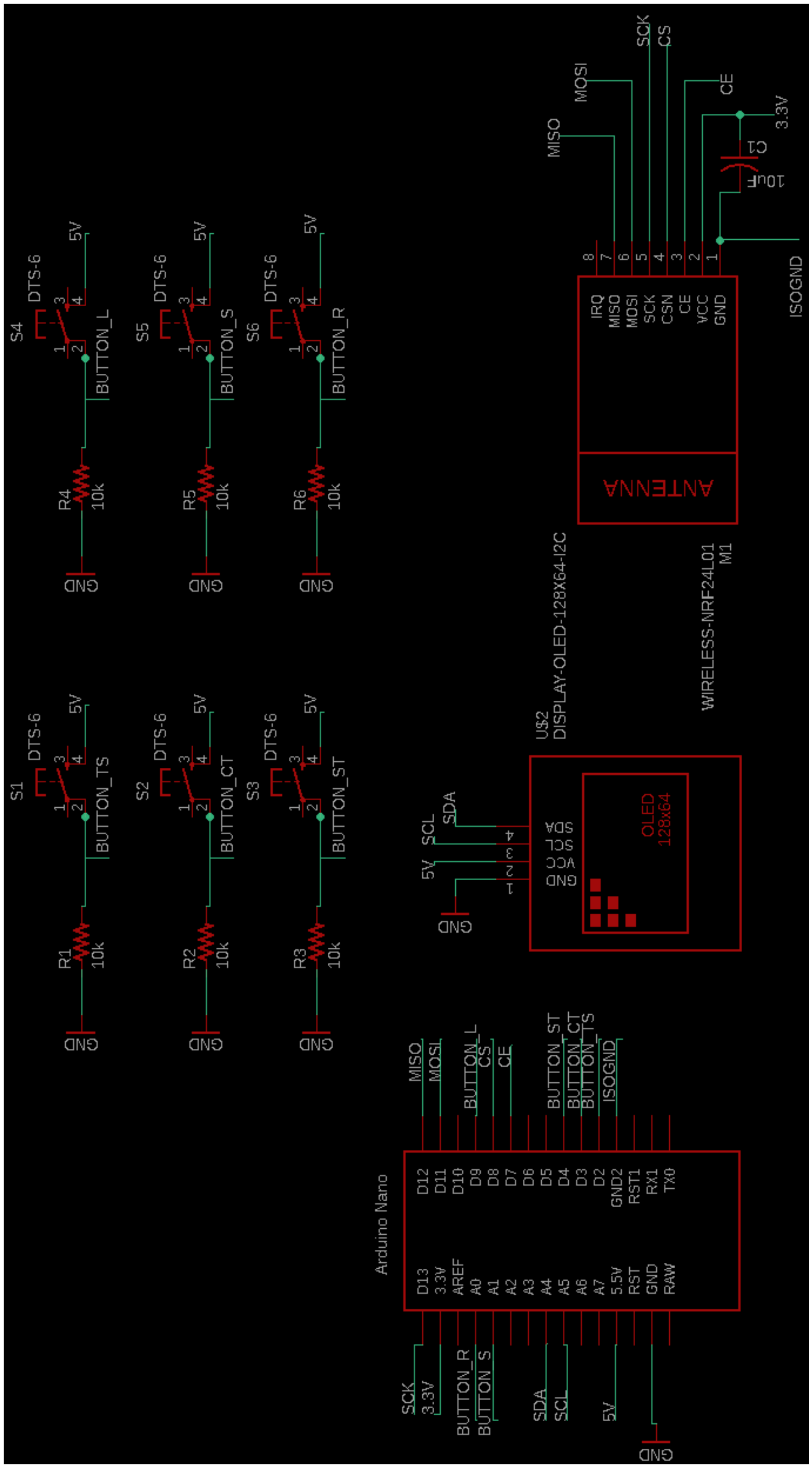

Fig. 16 Remote EAGLE Connection Diagram

B. Software Flowcharts

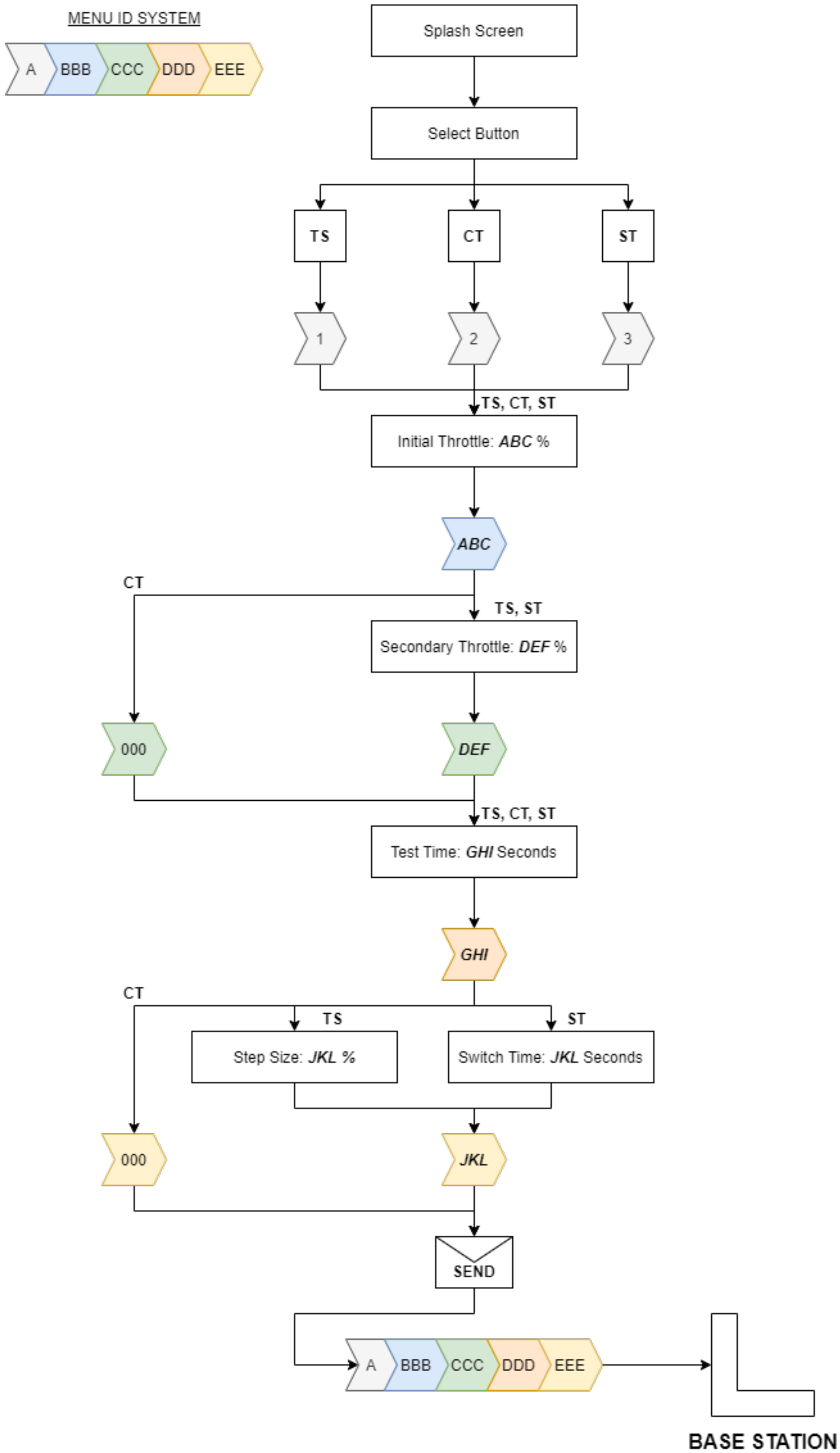

Fig. 17 Flowchart of Remote Software

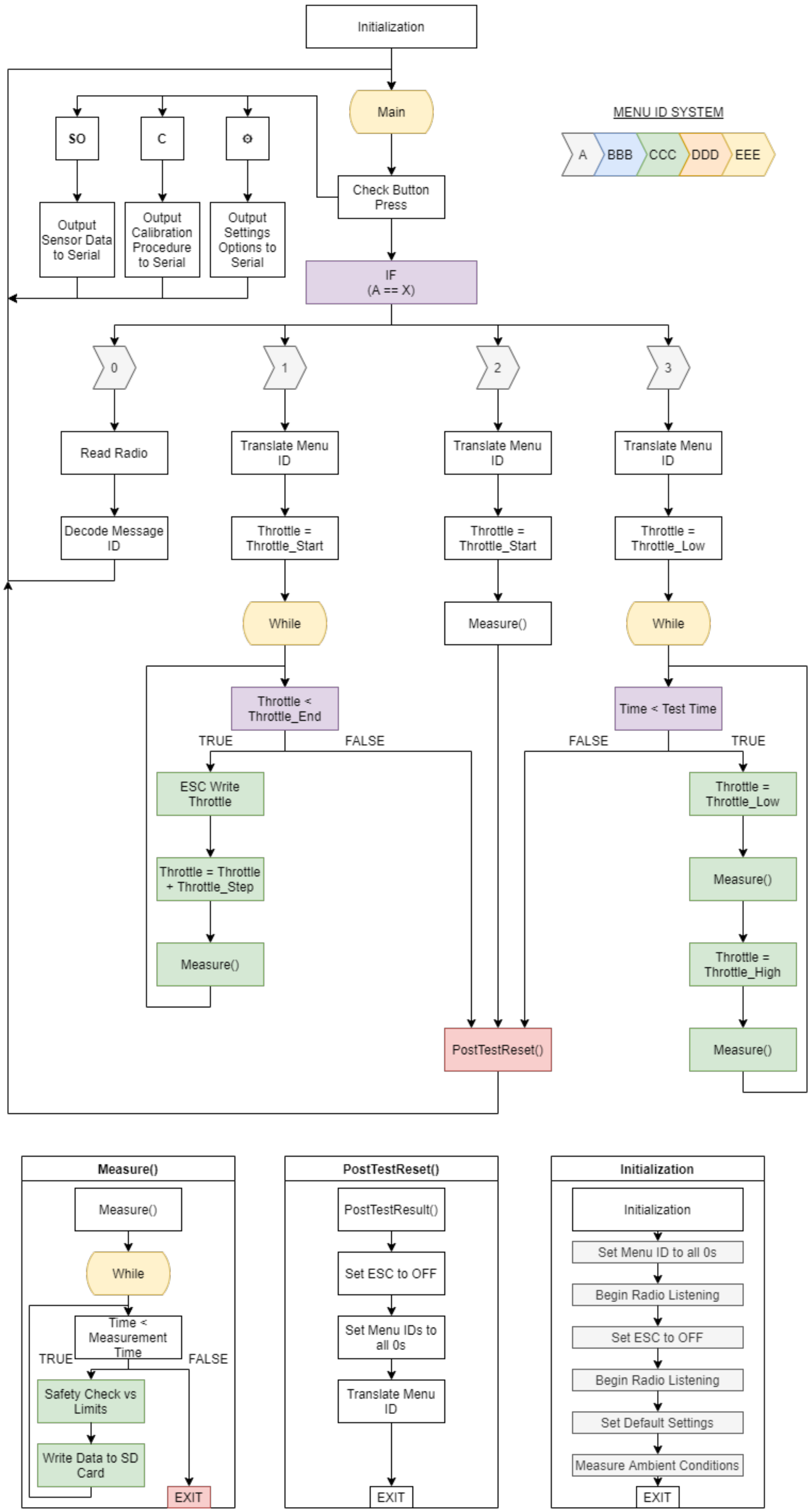

Fig. 18 Flowchart of Base Station Software

C. Sensor Calibration Procedures

To calibrate the thrust load cell we used a series of known weights ranging from 0 to 12.5 lbf for the short arm and 0 to 20 lbf for the long arm using a 0.5 lbf increment. We mounted the entire thrust stand vertically as shown in Figure 19. This removed the need for pulleys which could introduce additional friction and affect our measurements. To overcome the additional weight from the load cell structure, we recorded the unloaded output from the load cell to use as our tare. We performed the test 3 separate times to verify the repeatability of our sensor. To test the precision of the measurement, we ran 3 additional tests for small weights where we started unloaded and added weights in 0.02 lbf increments to check the linearity for small loads and found it to be capable of measuring 0.02 lbf increments reliably.

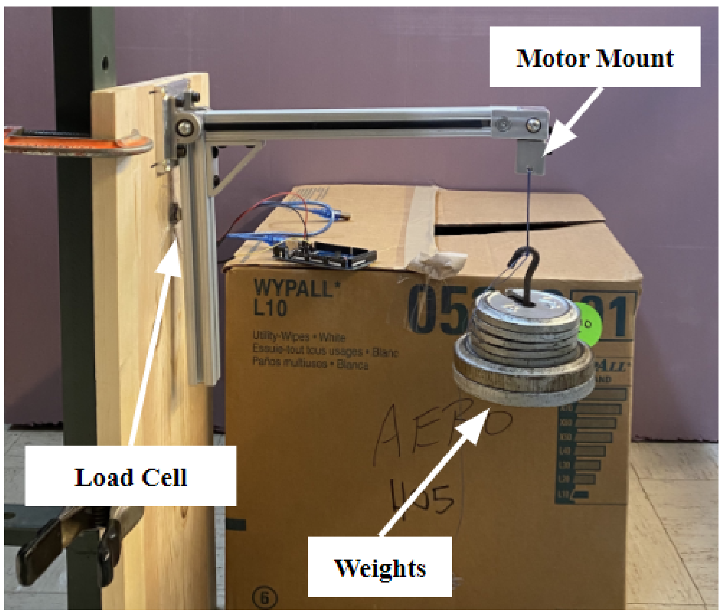

Fig. 19 Calibration setup for load sensor

To calibrate the torque sensor, we 3D-printed an arm to mount onto the motor mount of the torque sensor with holes located at 3 inches away from the rotation point. This allowed us to hang calibrated weights on a known moment arm as shown in Figure 20. We measured the torque in positive and negative directions loading from -15 lbf-in to +15 lbf-in incrementing by 1.5 lbf-in. This allowed us to generate a fit for the full range of our torque measurement in both directions. We also ran a test for small torques by incrementing by 0.06 lbf-in to determine our linear section and precision.

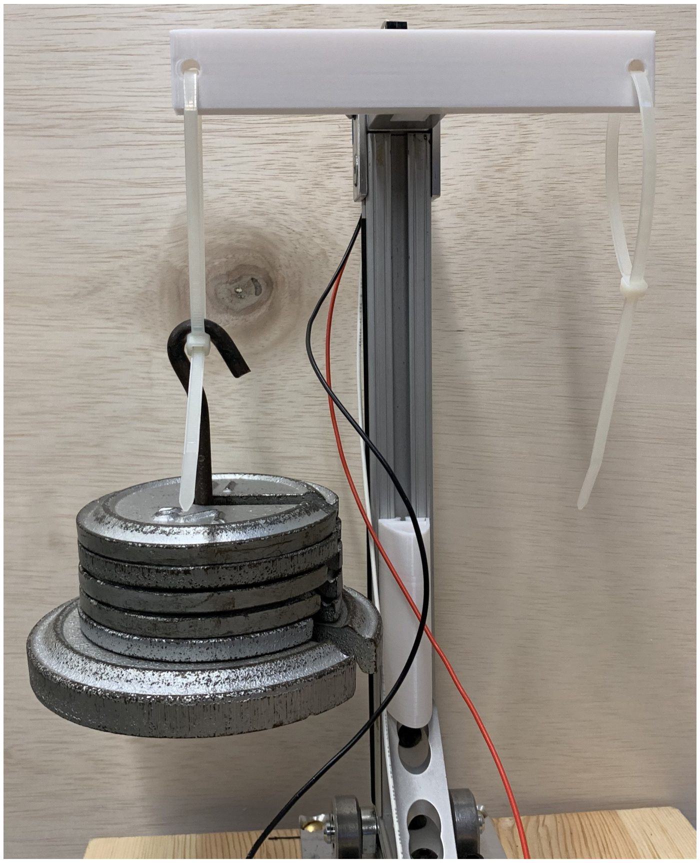

Fig. 20   Calibration setup for torque sensor

To calibrate the voltage sensor, we connected it to a variable power supply and increased the voltage in 1 V increments from 0 V to 25 V and recorded the output from the sensor. We maximized at 25 V since it is the voltage for a standard 6s Lithium-Polymer battery which is the largest we expect to be used on this thrust stand. By incriminating by 1 V, we were able to verify that the fit was linear throughout the entire range we expect to run.
To calibrate the current sensor, we connected the current sensor to a motor and calibrated ammeter. We ran the motor to a constant throttle and current, then recorded the current value from the ammeter and the output from our current sensor. We ran this through a range of throttle setting increasing by 5% to create a current fit. This method can be improved but due to lack of a large calibrated current source, this was our best option.

D. Static Testing Raw Data

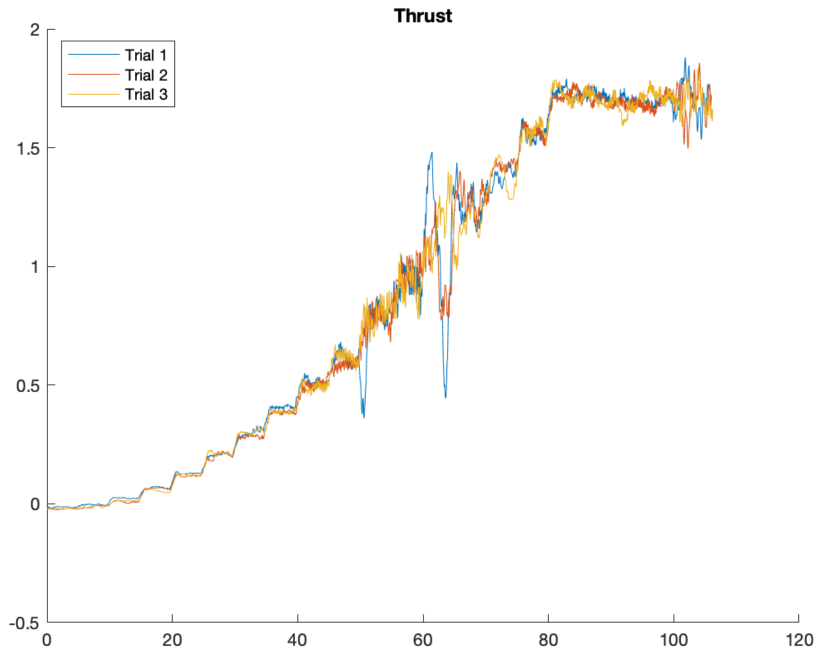

Fig. 21 Thrust Raw Data for 5.1x3.1x3 Propeller

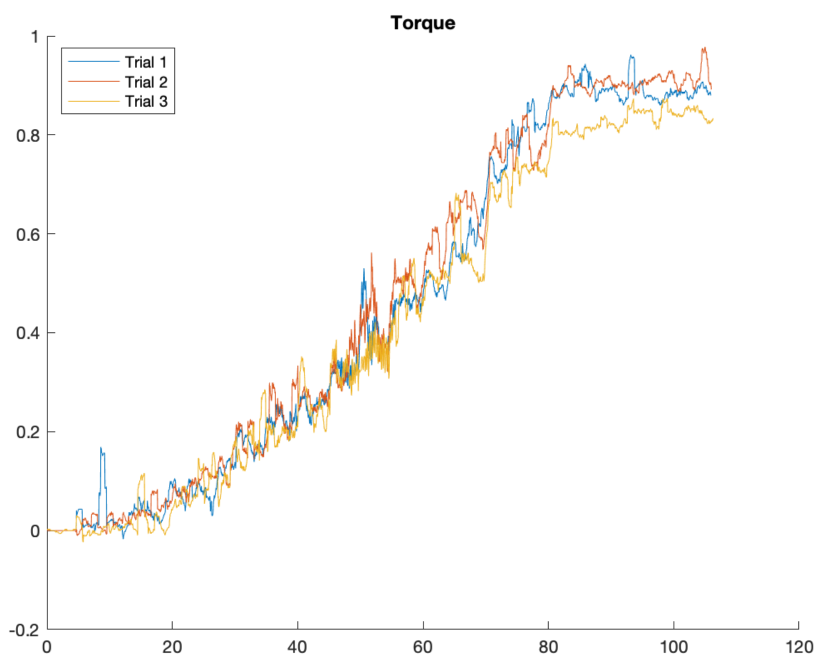

Fig. 22 Torque Raw Data for 5.1x3.1x3 Propeller

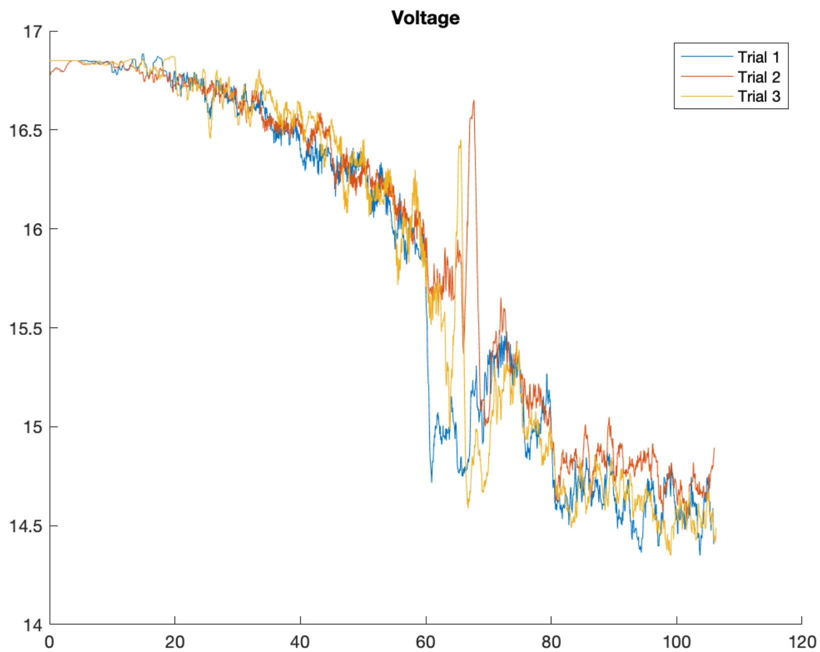

Fig. 23 Voltage Raw Data for 5.1x3.1x3 Propeller

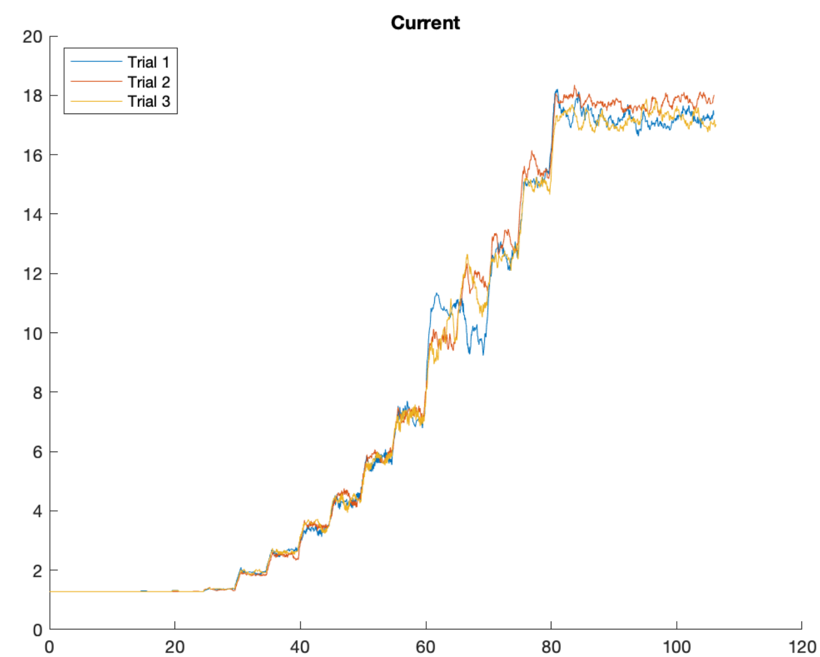

Fig. 24 Current Raw Data for 5.1x3.1x3 Propeller

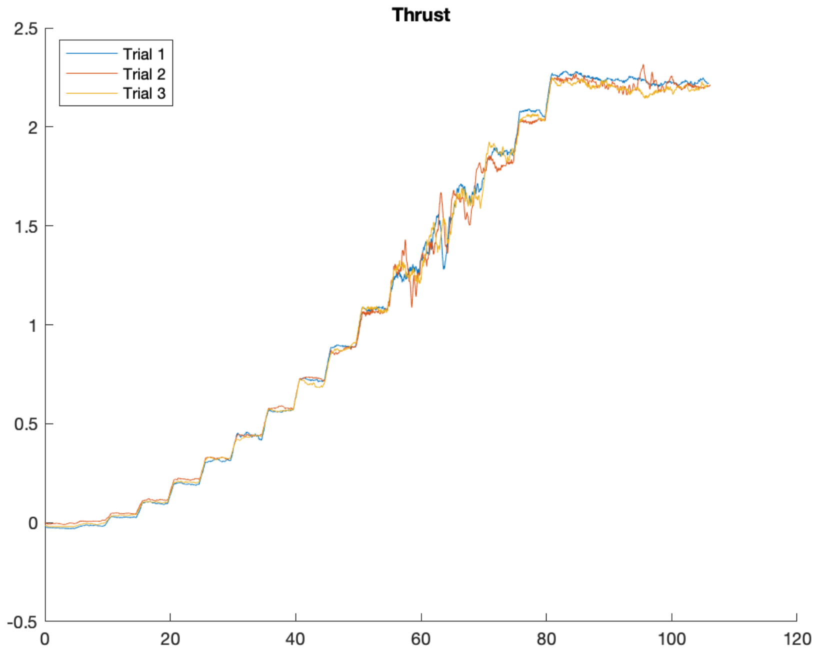

Fig. 25 Thrust Raw Data for 6x4 Propeller

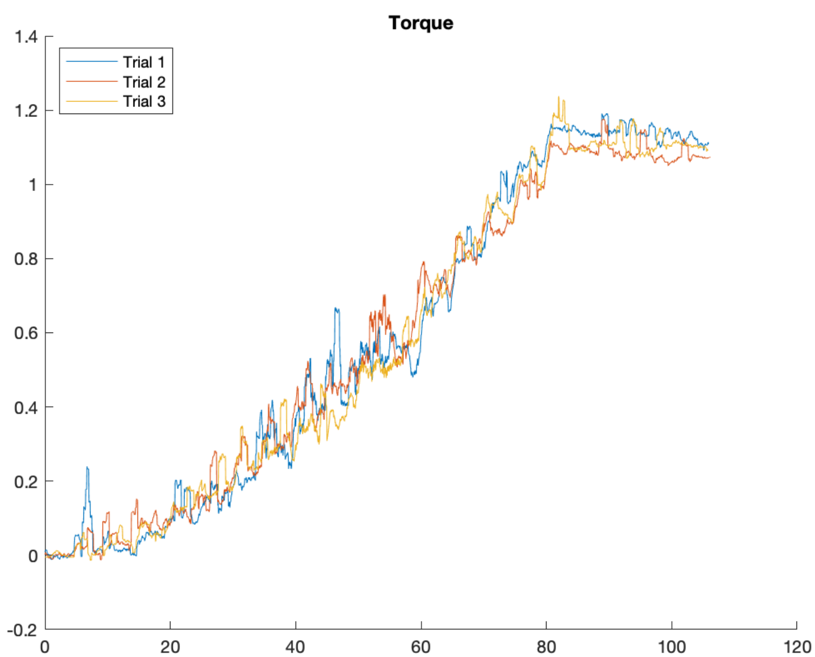

Fig. 26 Torque Raw Data for 6x4 Propeller

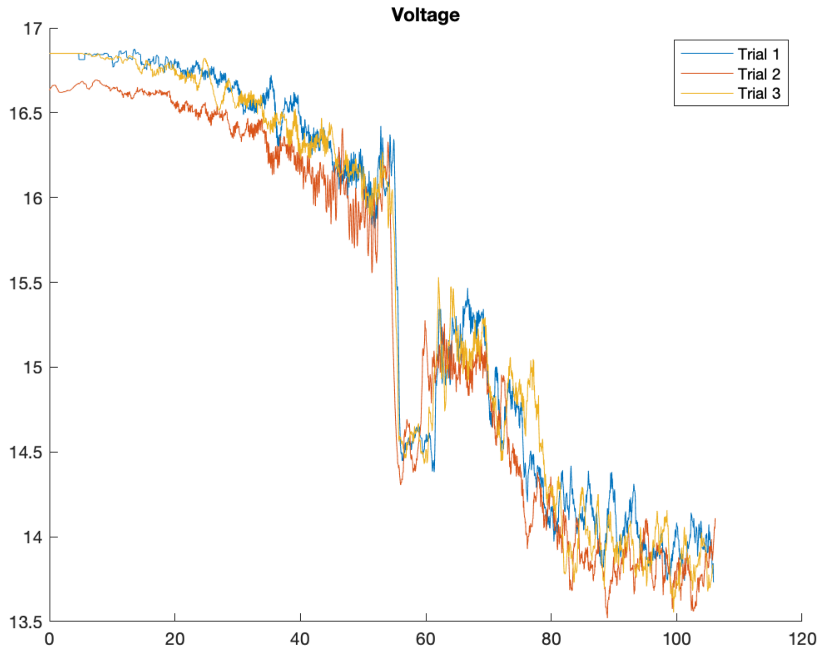

Fig. 27 Voltage Raw Data for 6x4 Propeller

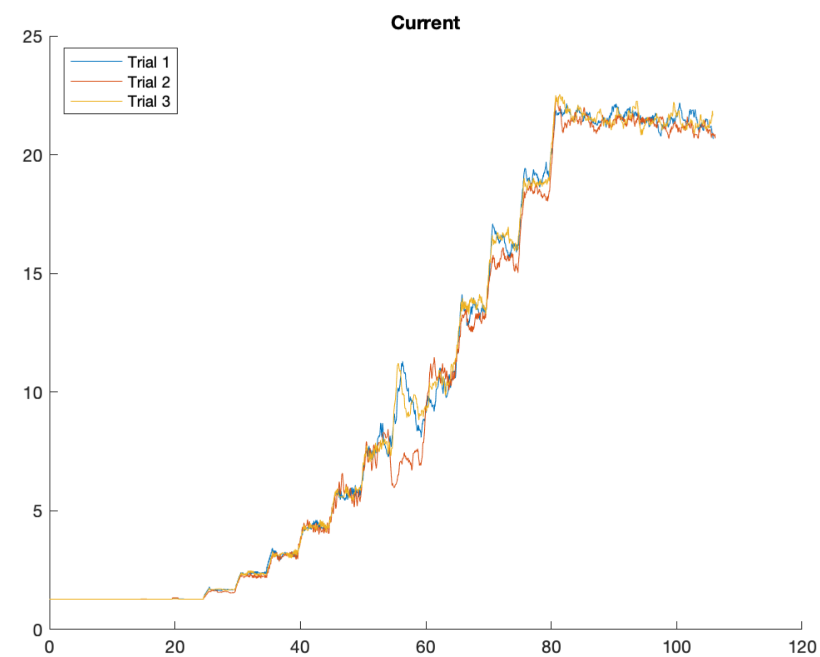

Fig. 28 Current Raw Data for 6x4 Propeller

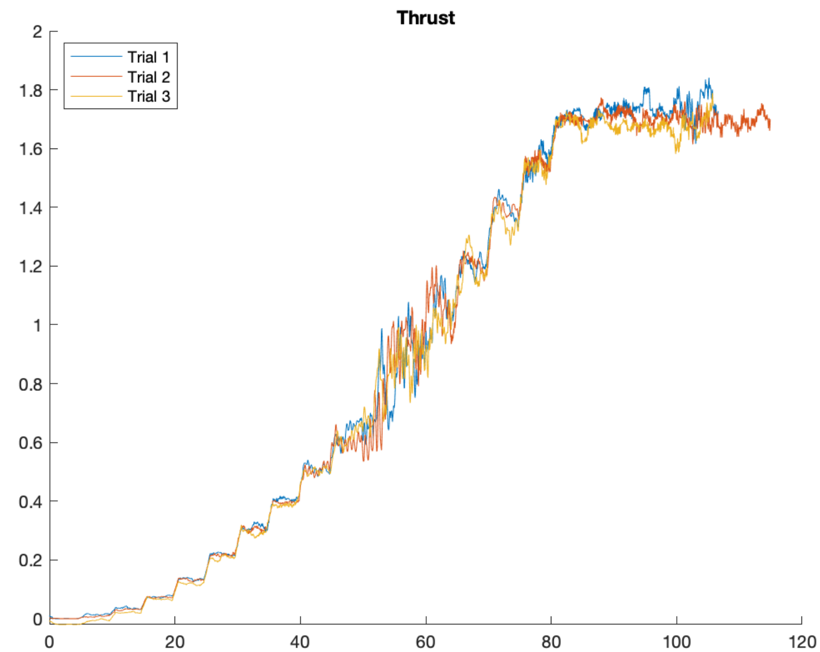

Fig. 29 Thrust Raw Data for 5x5.3x3 Propeller

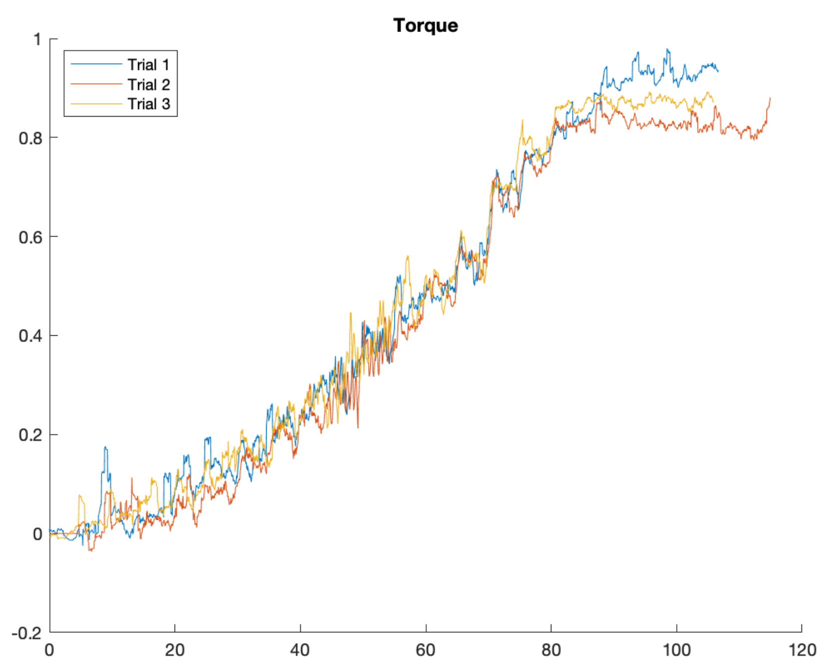

Fig. 30 Torque Raw Data for 5x5.3x3 Propeller

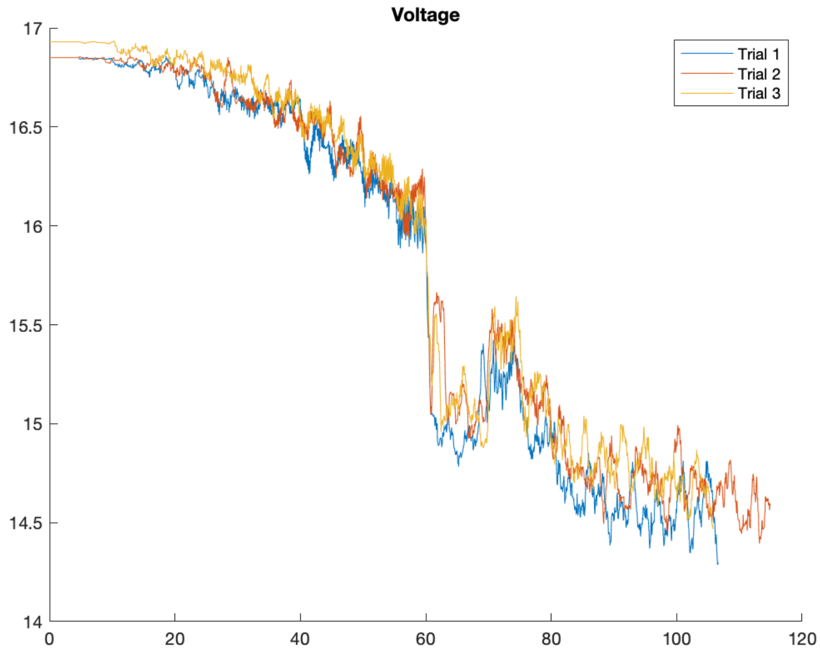

Fig. 31   Voltage Raw Data for 5x5.3x3 Propeller

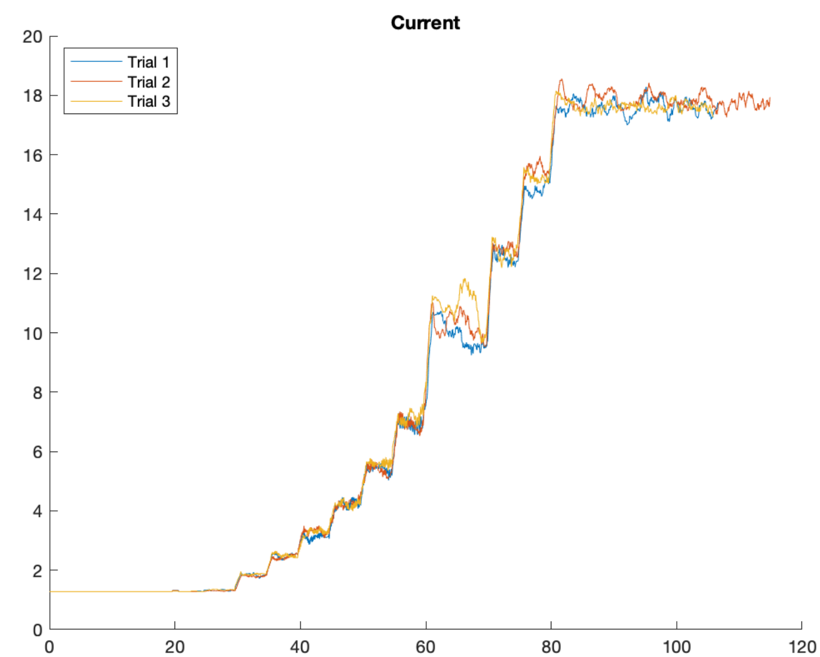

Fig. 32   Current Raw Data for 5x5.3x3 Propeller

E. Test Stand Images

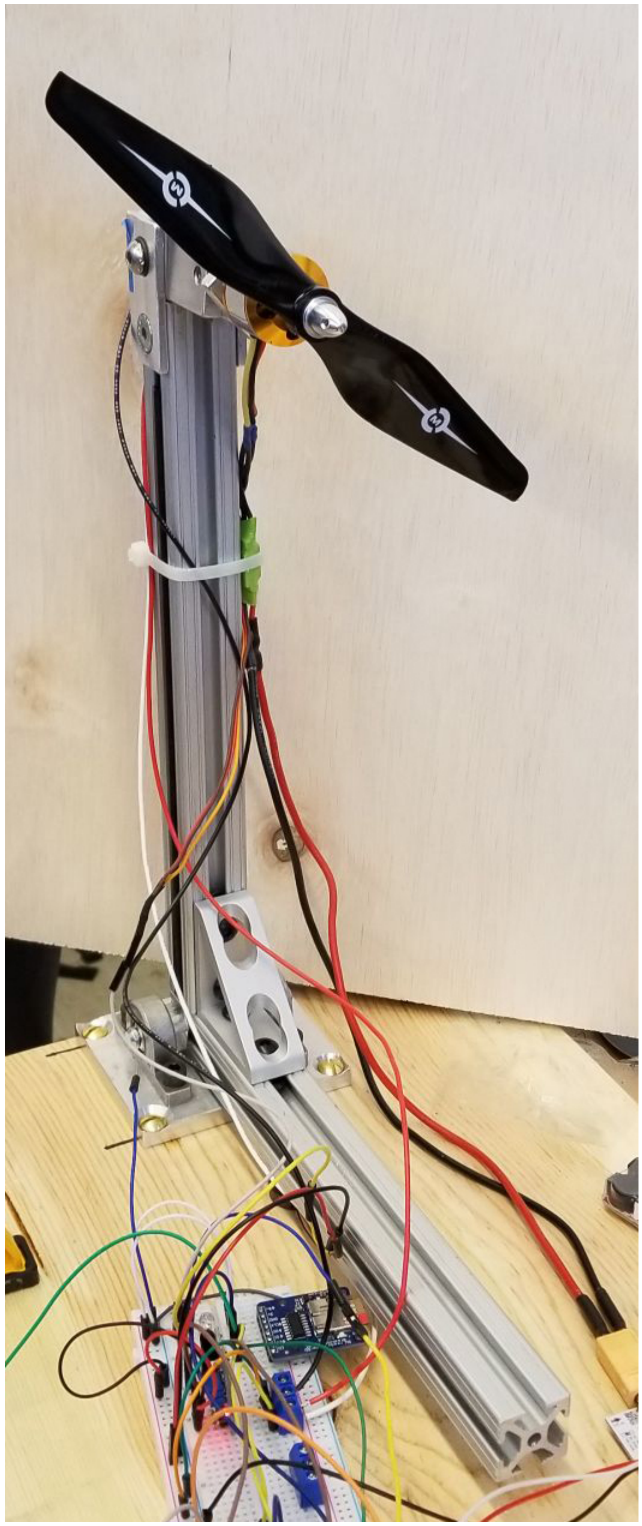

Fig. 33 Small Arm and Small Propeller

Fig. 34 Long Arm and Large Propeller